



LAWRENCE
LIVERMORE
NATIONAL
LABORATORY

Quarterly Technical Report, Fission Time Projection Chamber Project, July 2012

M. Heffner

October 4, 2012

Disclaimer

This document was prepared as an account of work sponsored by an agency of the United States government. Neither the United States government nor Lawrence Livermore National Security, LLC, nor any of their employees makes any warranty, expressed or implied, or assumes any legal liability or responsibility for the accuracy, completeness, or usefulness of any information, apparatus, product, or process disclosed, or represents that its use would not infringe privately owned rights. Reference herein to any specific commercial product, process, or service by trade name, trademark, manufacturer, or otherwise does not necessarily constitute or imply its endorsement, recommendation, or favoring by the United States government or Lawrence Livermore National Security, LLC. The views and opinions of authors expressed herein do not necessarily state or reflect those of the United States government or Lawrence Livermore National Security, LLC, and shall not be used for advertising or product endorsement purposes.

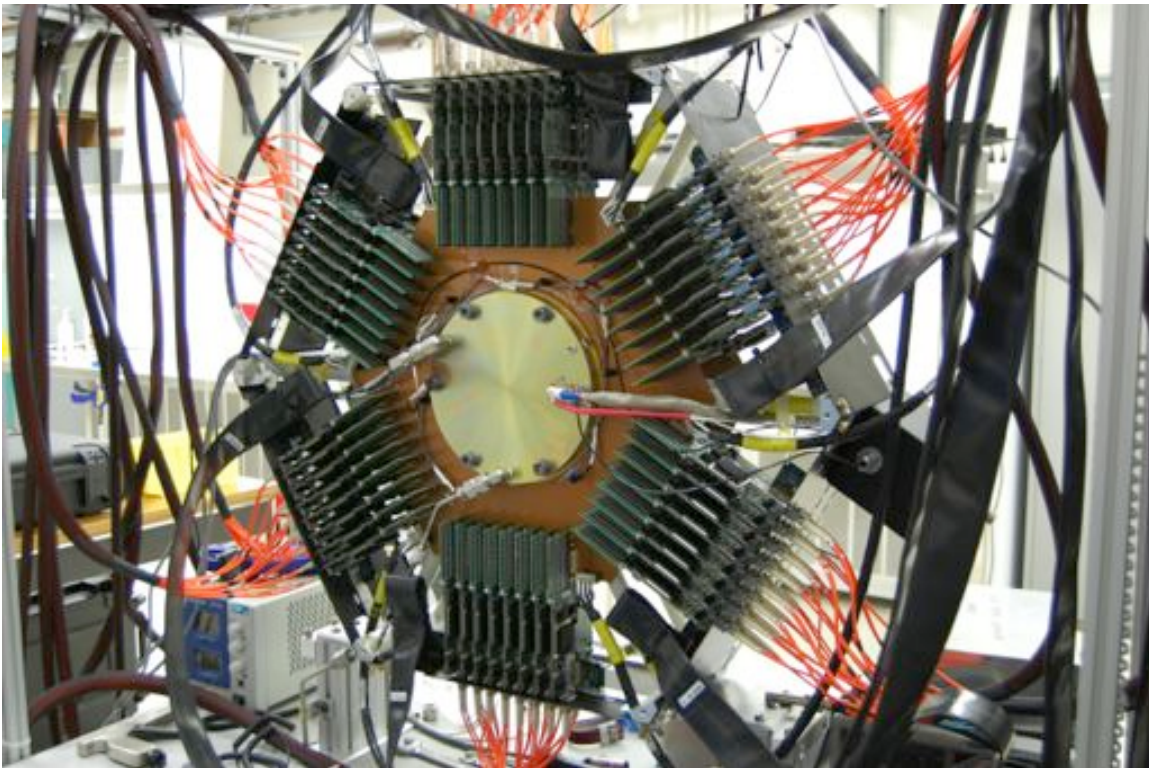
This work performed under the auspices of the U.S. Department of Energy by Lawrence Livermore National Laboratory under Contract DE-AC52-07NA27344.



July 2012

**Quarterly Technical Report
Fission Time Projection Chamber Project**

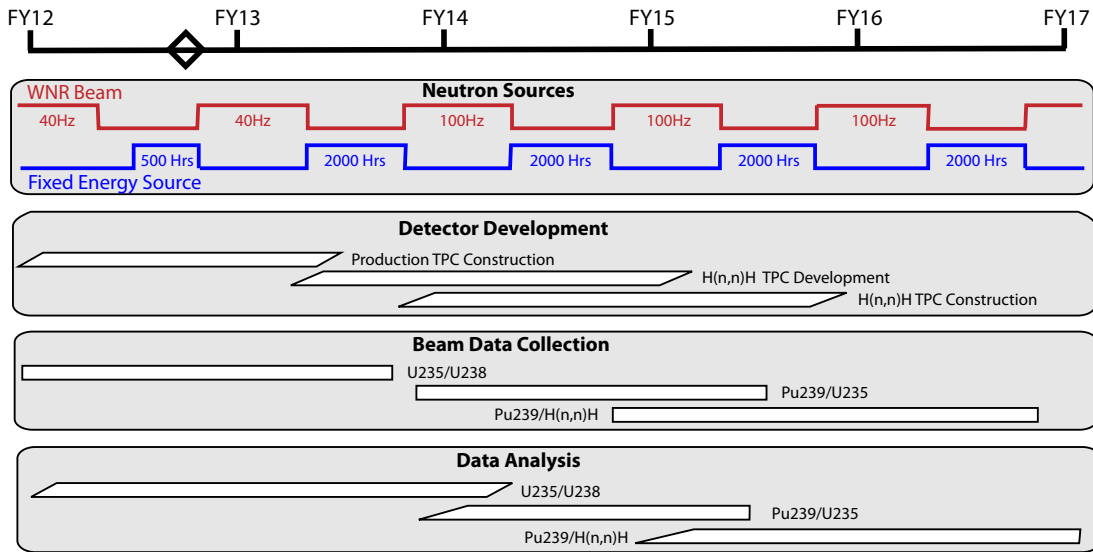
Collaborative Research Initiative



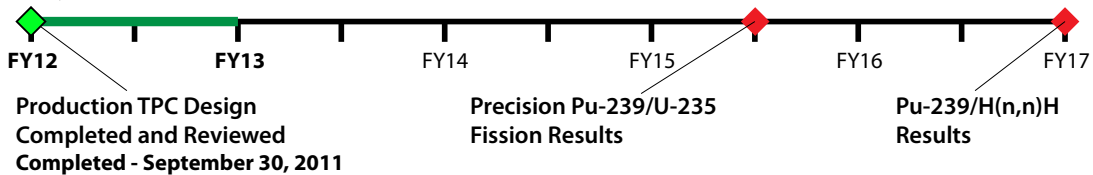
The Time Projection Chamber is a collaborative effort to implement an innovative approach and deliver unprecedented fission measurements to DOE programs. This 4π -detector system will provide unrivaled 3-D data about the fission process. Shown here is a half populated TPC (2π) at the LLNL TPC laboratory as it undergoes testing before being shipped to LANSCE for beam experiments.

Blank Page

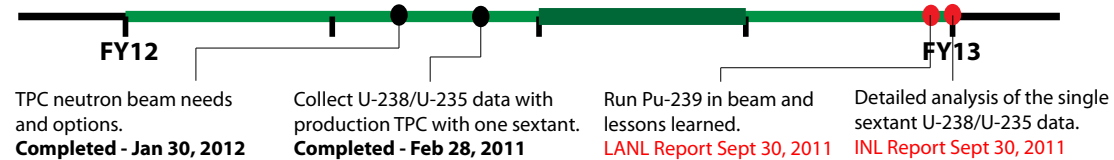
TPC Project Timeline



Major Milestones/Deliverables Timeline



FY12 Supporting Milestones/Deliverables



Third Quarter Highlights FY12

- The scale-up to half an instrumented TPC has been successful, including the integration of the high-speed cathode readout system. The system was tested at LLNL using Cm and Cf sources.
- The University funding was restored in this quarter after lengthy funding delays.
- A second Ph.D. was granted in the TPC project, to Lucas Snyder of the Colorado School of Mines, for his alpha to fission rate ratio measurement of Cf-252 using data from the single sextant configuration.

Potential Timeline Issues and Concerns

- Delayed funding for the University contract resulted in a lapse of support for several months last quarter. As a result, software development task efforts will be increased next quarter. University funding remains a challenge in reduced budget scenario with future funding unclear.
- 100 Hz operations at the LANSCE accelerator have not been recovered yet and the schedule is unclear.

Blank Page

Table of Contents

Principal Investigators	vi
Acronyms and Symbols	vii
Time Projection Chamber Project	11
Introduction.....	11
TPC Hardware [LLNL, CSM, INL, ISU, ACU]	12
Scope	12
Highlights.....	12
Time Projection Chamber [LLNL, CSM, INL]	12
Data Acquisition System [LLNL, ACU, ISU, INL]	16
Gas Handling and Temperature Control Systems [CSM, LLNL]	23
Target Design and Fabrication [OSU, INL].....	26
TPC Software [CalPoly, ACU, ISU, INL]	33
Scope	33
Highlights.....	33
Online Software [ACU]	33
Offline Software [CalPoly, ISU, INL, LLNL]	34
Data Acquisition Software [ACU, LLNL]	40
Simulation [CalPoly, ISU, LANL, PNNL]	42
Scope	42
Highlights.....	42
Data Analyses [CSM, LANL, CalPoly, ISU].....	49
Scope	49
Highlights.....	50
The Hydrogen Standard [OU]	58
Scope	58
Highlights.....	58
Facilities and Operation [LANL, LLNL, OU].....	58
Scope	59
Highlights.....	59
Livermore [LLNL].....	59
Los Alamos [LANL]	60
Ohio University [OU]	63
Management.....	64

Principal Investigators

Universities

NE funded

E. Burgett	Idaho State University
J. Klay	California Polytechnic State University, San Luis Obispo
R. Towell	Abilene Christian University
D. Isenhower	Abilene Christian University
U. Greife	Colorado School of Mines
W. Loveland	Oregon State University
S. Grimes	Ohio University
T. Massey	Ohio University

Laboratories

NE, NNSA funded

T. Hill	Idaho National Laboratory
M. Heffner	Lawrence Livermore National Laboratory
F. Tovesson	Los Alamos National Laboratory
D. Asner	Pacific Northwest National Laboratory

Acronyms and Symbols

ACU	Abilene Christian University
AFCI	Advanced Fuel Cycle Initiative
AFM	Atomic Force Microscopy
Am	Americium
ANL	Argonne National Laboratory
ANS	American Nuclear Society
ASME	American Society of Mechanical Engineers
Atm	Atmosphere (pressure unit)
Ba	Barium
Be	Beryllium
Bi	Bismuth
BNL	Brookhaven National Laboratory
CalPoly	California Polytechnic State University, San Luis Obispo
Ce	Cerium
Cm	Curium
CS	cross section
Cs	Cesium
CSM	Colorado School of Mines
Cu	Copper
CVD	Chemical Vapor Deposition
DANCE	Detector for Advanced Neutron Capture Experiment
DAQ	Data Acquisition System
DOE	Department of Energy
dpa	Displacements per Atom
EIS	Environmental Impact Statement
ENDF	Evaluated Nuclear Data File - Evaluations that can be used in MCNPX for more accurate predictions of fission, criticality, transport, and radiation damage
ES&H	Environmental, Safety, and Health
Eu	Europium
Fe	Iron
FPGA	Field-programmable gate array
FWHM	Full Width Half Maximum
GEANT4	Geometry And Tracking monte carlo program from CERN
GIT	Georgia Institute of Technology
GNASH	Nuclear Reaction Code
H	Hydrogen
He	Helium
HEU	Highly enriched uranium
Hf	Hafnium
Hg	Mercury
IAC	Idaho Accelerator Center
IAEA	International Atomic Energy Association (Vienna, Austria)
IFR	Integral Fast Reactor
INL	Idaho National Laboratory
ISTC	International Science and Technology Centre (Moscow)
ITU	Institute for Transuranium Elements (Karlsruhe, Germany)
JAERI	Japan Atomic Energy Research Institute
JLAB	Jefferson Laboratory (VA)
K	Potassium
keV	Kiloelectron Volt
Kr	Krypton

LA150n	Los Alamos generated nuclear data library, extending up to 150 MeV
LAHET	Los Alamos High-Energy Transport
LANL	Los Alamos National Laboratory
LANSCE	Los Alamos Neutron Science Center
LLFP	Long Lived Fission Products
LLNL	Lawrence Livermore National Laboratory
MA	Minor actinide
mb	Millibarn
mCi	Millicurie
mips	Minimum ionizing particles
MCNP	Monte Carlo N-Particle Transport Code
MCNPX	Merged code—Los Alamos High-Energy Transport (LAHET) and Monte Carlo N-Particle Codes (MCNP)
mL	Milliliter
Mo	Molybdenum
MOX	Mixed-oxide fuel
mR	Millirad (a measure of radiation)
N	Nickel or nitride
Np	Neptunium
NEA	Nuclear Energy Agency (Paris)
NEPA	National Environmental Protection Agency
NERAC	Nuclear Energy Research Advisory Committee
NERI	Nuclear Energy Research Initiative
NIFFTE	Neutron Induced Fission Fragment Tracking Experiment (TPC Collaboration name)
O	Oxygen or Oxide
O&M	Operations and Maintenance
ORNL	Oak Ridge National Laboratory
OSU	Oregon State University
OU	The Ohio University
PACS	Personnel Access Control System
Pb	Lead
Pd	Paladium
PNNL	Pacific Northwest National Laboratory
Pu	Plutonium
PUREX	Plutonium-Uranium Extraction
QA	Quality Assurance
R	Rad (a measure of radiation)
rms	root mean square
ROOT	an object oriented data analysis framework from CERN
RSICC	Radiation Safety Information Computational Center
Ru	Ruthenium
SEM	Scanning Electron Microscopy
SNF	Spent Nuclear Fuel
SNL	Sandia National Laboratory
SRS	Savannah River Site
STP	Standard Temperature and Pressure
Ta	Tantalum
Tc	Technitium
TEM	Transmission Electron Microscopy
TJNAF	Thomas Jefferson National Accelerator Facility
TPC	Time Projection Chamber
TRL	Technical Readiness Level
TRU	Transuranics (americium, curium, neptunium, and plutonium)
TRUEX	Aqueous solvent extraction process for TRU recovery

U	Uranium
UREX	Uranium Extraction (an aqueous partitioning process)
V	Vanadium
W	Tungsten
WBS	Work Breakdown Structure
WNR	Weapons Neutron Research (facility at LANSCE)
Xe	Xenon
Y	Yttrium
Zr	Zirconium

Blank Page

Time Projection Chamber Project

Introduction

Reactors, weapons and nucleosynthesis calculations are all dependent on nuclear physics for cross sections and particle kinematics. These applications are very sensitive to the nuclear physics in the fast neutron energy region and therefore have large overlaps in nuclear data needs. High performance computer codes interface the nuclear data through nuclear data libraries, which are a culmination of experimental results and nuclear theory and modeling. Uncertainties in the data contained in those libraries propagate into uncertainties in calculated performance parameters. The impact of nuclear data uncertainties has been studied in detail for reactor and weapon systems and sensitivity codes have subsequently been developed that provide nuclear data accuracy requirements based on adopted target accuracies on crucial design parameters. The sensitivity calculations have been performed for a number of candidate systems. These sensitivity studies provide specific requirements for uncertainties on many fission cross sections, many of which are beyond the reach of current experimental tools. The sensitivity codes are proving to be very useful for identifying the highest impact measurements for DOE programs and the TPC measurement program will help provide those data. The result of these new, high-accuracy precision measurements will be a refined understanding of performance results, thus reducing the liability nuclear data has on the overall uncertainties in calculated integral quantities. The new class of high-accuracy, high-precision fission measurements will not be easy. The proposed method is to employ a Time Projection Chamber and perform fission measurements relative to H(n,n)H elastic scattering. The TPC technology has been in use in high-energy physics for over two decades - it is well developed and well understood. However, it will have to be optimized for this task that includes miniaturization, design for hydrogen gas, and large dynamic range electronics. The TPC is the perfect tool for minimizing most of the systematic errors associated with fission measurements. The idea is to engineer a TPC specifically for delivering fission cross section measurements with uncertainties below 1.0%.

The long term goal is to fill the TPC with hydrogen gas and measure fission cross sections relative to H(n,n)H elastic scattering, thus removing the uncertainties associated with using the U-235 fission cross section for normalization. In fact, we will provide the world's best differential measurement of the U-235 fission cross section and this will impact nearly all fission library data, since it has been used as a standard in much of the available fission experimental data.

The immediate objective of this effort is to implement a fission cross section measurement program with the goal of providing the most needed measurements with unprecedented precision and accuracy using a time projection chamber. The first three years of this program will provide all the groundwork and infrastructure for a successful measurement campaign. Shortly following, we will provide precision fission ratio measurements for Pu-239/U-235 and U-238/U-235 along with a full design proposal to measure $^{235}\text{U}/n(n,p)p$. The $^{235}\text{U}/\text{H}(n,n)\text{H}$ measurement will provide the best single measurement of the U-235 fission cross section and will allow us to convert the initial, and any subsequent, ratio experiments to world's best absolute measurements. After completion of the U-238 and Pu-239 ratio measurements, the experimenters will move on to measurement of the minor actinide cross section,

fission fragment distribution and neutron yield measurements. This information will play a crucial role in the long term DOE nuclear R&D campaign.

The reporting for this project is broken down into seven categories:

- TPC Hardware activities include design, testing and operation of the complete time projection chamber, including gas system and electronics.
- TPC Software activities will provide the project with the required programming for the online data acquisition system, data reduction and analysis as well as simulation.
- Simulation activities will provide the project with the required simulations of the physics and detector response through the entire electronics chain.
- Data Analysis activities will demonstrate the TPC performance through the entire software chain.
- The Hydrogen Standard will be used to minimize total cross section errors. The ability to accurately and precisely determine fission cross sections hinges on the H(n,n)H total cross section and angular distributions.
- Facilities and Operations will need to be identified and prepared for the construction, testing and operation of the TPC. This activity is spread amongst the collaborators, based on the work they are performing, such as target fabrication, computing, design, component testing, and operation.
- Management section describes the organizational work required for a project this size.

TPC Hardware [LLNL, CSM, INL, ISU, ACU]

Scope

The components that make up the TPC proper are included in this section. This includes the pressure vessel, field cage, pad-plane, gas amplifier, laser alignment system, targets, electronics and the engineering required to integrate all of the parts into a working system.

Highlights

- This quarter marks a major accomplishment in the aggressive schedule for the TPC project. For the first time, a full pad plane has been instrumented, tested and operated at the LLNL TPC laboratory.
- The TPC has been shipped to LANSCE for beam experiments at the dedicated 90L flight path during the upcoming run cycle.
- The experiment can now be completely controlled from a remote internet location using the specially adapted MIDAS package.
- All necessary targets have been prepared and shipped to LANL for the upcoming experiments.

Time Projection Chamber [LLNL, CSM, INL]

The TPC is the centerpiece of the experiment and consists of a number of parts and systems that are being designed and integrated into a working whole. All subsystems

that support the operation of the chamber are either complete or nearing completion, where much of what is left are refinements and integral testing. Partially instrumented versions of the TPC have been used to successfully collect radioactive source data at LLNL and beam induced reactions at LANSCE that demonstrate the level of readiness for production running. This evolutionary approach has provided the design team with valuable performance information as feedback for final experimental design requirements. This section will describe the progress on each of those efforts.

Current Implementation

This quarter marks a major accomplishment in the aggressive schedule for the TPC project. For the first time, a full pad plane has been instrumented, tested and operated at the LLNL TPC laboratory (shown in Figure 1). This implementation allows for complete reconstruction of all charged particles in one half of the sensitive gas volume. This configuration is a complete test of the complete electronic infrastructure required for production running. This accomplishment required 92 EtherDAQ/preamplifier card pairs operating together (~3000 channels) through several supporting architectures, evenly distributing power and precision clock signals in a coordinated way and debugging many of the issues expected with a complex, high-density, custom electrics system of this size. The other half of the TPC is simply a mirror image of the currently instrumented side where other than refinements, the further concerns that will need to be addressed in the months to come are total power consumption, thermal and data flow management.

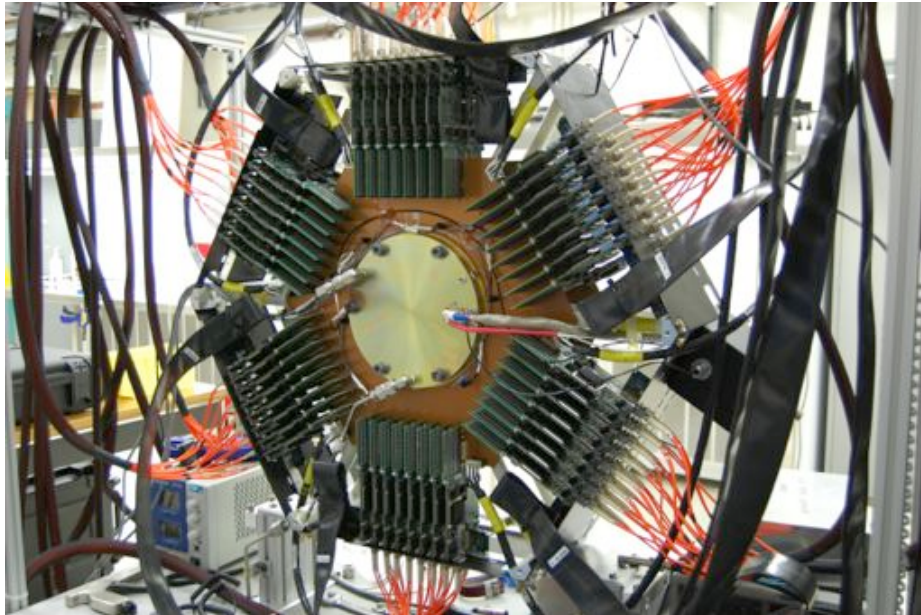


Figure 1: Here is the TPC at LLNL loaded with all 92 cards needed to operate one full pad plane, or one half of the detector. There are approximately 3000 channels instrumented in this photo.

The fully tested TPC has been packed and shipped to LANL for installation and subsequent operation during the next LANSCE run cycle, which begins in August.

Cathode Pad plane

Version 3 of the pad plane was designed and built last quarter. This version has improvements to the glue down region for the micromesh and more importantly is setup for robotic placement of the 96 connectors that go on each board. They were inspected for correct pillar height and some other preliminary inspections, and then sent to the loading shop for connector placement (see Figure 2).

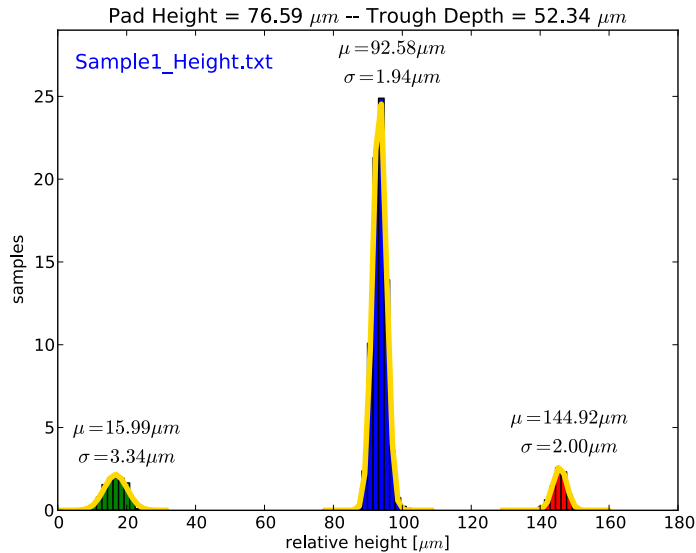


Figure 2: Shown here is the pad plane profilometry measurement summary revealing the consistency of construction.

The 12 new pad planes constructed the last quarter have all of the modification identified during the testing last year. In order to meet the goal of a fully instrumented pad plane we needed to load all 92 connectors attached to the pad plane, which is a large job given that each connector has 80 pins and they have a pitch of 0.4mm. The boards were sent to a component load shop for this work and they had problems that prevented us from getting a full set of working boards, but we did have one that worked well. There were some shorts on the connectors and we replaced them by hand. The result was a single fully functioning pad plane. We will revisit the auto loading of the connectors with a different company once we field the TPC at LANL. All of the pad plans that we used were carefully inspected both electrically and optically to look for defects.

Field Cage

Three Field cages were constructed and shipped to LANL for the upcoming runs at LANSCE. Each field cage holds one target and they can be swapped out as a single unit, minimizing the handling of fragile targets. We are planning on using a variety of targets at LANL during this run cycle and the field cage units will allow us minimize the time to swap them out and reduce the chances of breakage.

Electronics Cooling

The EtherDAQ/preamplifier card pairs consume enough power that cooling is essential for their proper operation. A convection system based on 36 standard electronic fan packs electronics has been designed to cool the 192 card pairs (see). These fans were mounted on the TPC shield, which serves both as an EMF shield and air flow deflector. The power supply for the fan system was integrated into the run control for the experiment.

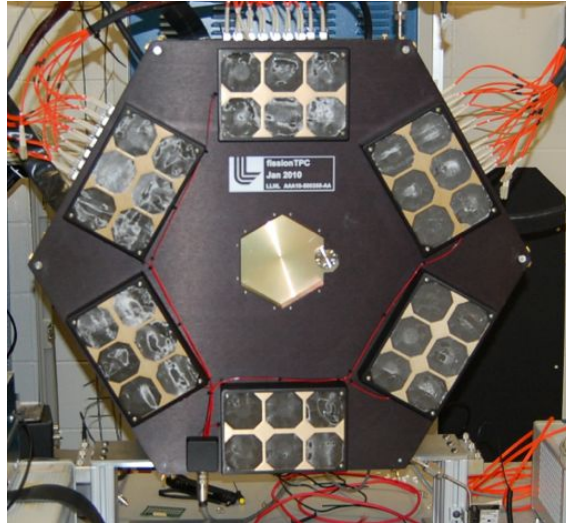


Figure 3: Shown here is the TPC shield that surrounds the gas chamber with the cooling fans attached. The single power connection is at the lower left and power is distributed across the face to each of the 6 packs of 6 fans that direct air over the EtherDAQ/preamplifier card pairs.

High Speed Cathode Readout (HiSCaR)

The High Speed Cathode Readout (HiSCaR) is the electronics that will allow the TPC experiment to determine the incident neutron energy that causes a charged particle reaction (fission, (n,p) scattering, etc.). The precise HiSCaR timing signal is used in conjunction with the LANSCE accelerator timing signal to measure the neutron time of flight to derive the energy. This is a difficult measurement since in the end, we will need a fast signal with extremely low noise to pickup the proton signals. A shielding and grounding plan has been developed to minimize the noise and pickup that is difficult to remove. For example the 25MHz clock to the TPC does make it into the signal at some level. We have a plan to improve this and this version is just a quick start so we have a signal for the first running of the full pad plane. The boxes that accomplish this measurement have been built, tested and shipped to LANL for installation

Laser Alignment System

The laser calibration system for the TPC is important to measure field distortions caused by positive ions in the drift gas. The first design was to use a fiber to transport the laser beam from the laser head to the pressure vessel and down optical rods with prisms at the ends. After a number of attempts to use a fiber we found that

it simply can not handle the power. We have decided to change the design to match closer to a proven design used in the STAR TPC experiment. A conceptual design of the TPC laser system has been completed, and work has started on the details of constructing that design. The first difficult problem is mounting and carefully aligning the very small (1mm) and fragile glass rods. It was determined that a small flat ground into the glass could be used with a fixture to align the rods and then epoxy them in place. The alignment fixture has been designed, and the next step is to test this procedure.

Data Acquisition System [LLNL, ACU, ISU, INL]

The TPC will have over 6000 pads, each of which need to be instrumented with a preamplifier, ADC and digital readout. The challenge of a large number of densely packed high-speed channels has been met in the past with custom ASIC chips. The technology of both ADC and FPGA has improved considerably over the last decade and it is now possible to use off-the-shelf components to accomplish the same task for considerably less development cost, less time to working prototypes, and considerably more flexibility in the final design.

Preamplifier Cards

It was observed at LANSCE that the micromegas was not as stable as the operations at LLNL. The discharges happen every few days or so, and each time the discharge hits a preamp it kills the preamp fet (~\$1 part) that is difficult to replace in the field. We think the discharges are the result of dust entering the TPC and the environment at LLNL is substantially cleaner than at LANSCE. We are working to clean up the work area at LANSCE and also working to make the preamps more robust against sparking. A prototype for the protection circuit was designed and tested. It was tested both for the ability to withstand sparks, and that it does not increase the noise of the system. The PCB was modified and is ready for production. We don't currently have the funds to make this run so we are holding off for now. We will use the older unprotected preamps for the next run cycle.

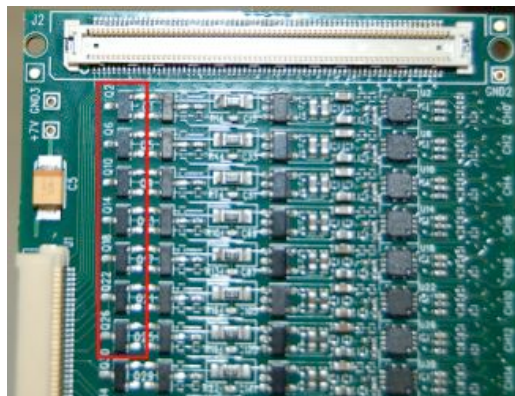


Figure 4: The FETs that are damaged by sparking in the TPC.

EtherDAQ Cards

Over half of the production electronics were built this quarter. There was a significant problem found with the soldering of the production EtherDAQ cards. It looks like from the x-ray that the pad on the bottom of some chips was not soldered. We visited the assembly shop to diagnose this problem. A similar problem with soldering may also effect about 6 or the 30 digital bus board cards. In this case, it is a smaller problem since there are fewer needed cards, they are easier to repair, and they cost less. The problem was resolved at the pick-and-place shop by having them rework all of the boards. The end result was that we all but a few to pass which is an excellent yield. A production run of 80 EtherDAq board was also completed last quarter. After receiving the cards they were inspected, tested and programmed. In this quarter, we tested and programmed over 100 EtherDAQ cards and were placed into service.

When operating a large number of EtherDAQ cards we noticed that sometimes the cards would not obtain a necessary Ethernet link. This issue was debugged and solved with a modification to the FPGA firmware.

A separate problem with the electronics is that they would sometimes fall into a mode where they stopped working. We found that this was correlated with the quality of the clock that was distributed to all cards to keep them in sync. The power and clock distribution unit (PCDU) is a custom box was modified to change the clock from a simple TTL signal to a differential LVDS format. This improved the clock and the failure mode of the electronics has not reappeared. We will continue to investigate in the firmware why this was happening, but this fix will allow the experiment to continue. The modified PCDU was shipped to LANL for in-beam runs.

High Voltage System

The gain stage of the TPC requires careful filtering of the high voltage power and also needs a very sensitive trip circuit to prevent damage to the TPC in the event of a discharge. This is accomplished with the custom filter box that we designed. This has operated very well and a second one was constructed for operation at LANL and has been shipped.

HiSCaR

The cathode of the TPC can be instrumented to determine the time-of-flight of neutrons arriving at the TPC. This is used to determine the energy of the neutrons to make the cross section measurement. This system consists of two parts. The first is an analog amplifier that takes the small signal from the cathode, amplifies it and conditions it for recording by a digital system. This amplifier has to be fast and low noise which is difficult to accomplish simultaneously. A first version of this amplifier has been built and we are working to refine it. The second part is the digital readout. This is complicated by the fact that we need the timing with respect to the master TPC clock. We have solved this by using a TPC card and making a special interface card that takes the signal from the preamp and delays it 20 times each for just 1 ns. The delayed signals are fed into 20 channels and from this we can get very good timing. This part has been tested with a pulser and works well. This quarter we have integrated the two parts and we now have a higher speed readout of fission at the cathode. This was done at LLNL with a 252Cf source. The rise time is limited by the

cable capacitance at the front end and is currently 300-400ns. This is too long, but will be used to get started in the next run cycle. Working with a pulser, it looks like 10-20ns rise is possible once the amplifier is placed inside the TPC; something we plan to have by at least the run cycle in CY13.

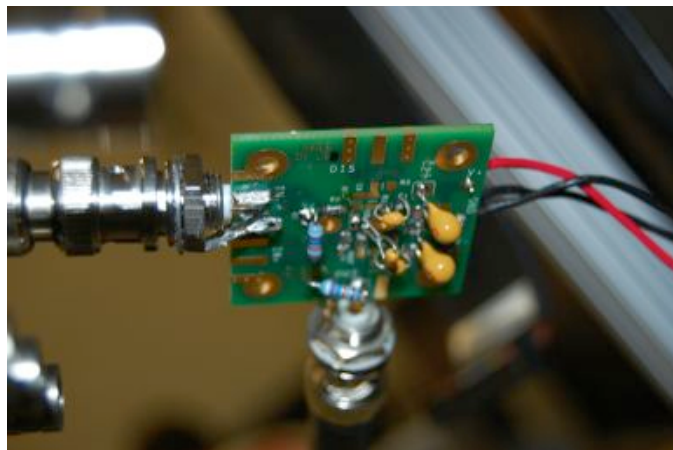


Figure 5: Prototype preamp used on the TPC cathode.



Figure 6: Delay board used to get high speed timing with the TPC electronics need to get the signal readout on the TPC timebase.

Power and Clock Distribution

The power and clock distribution system (PCDU) is shown in Figure 7 was completed for 6 channels and tested. This allows for operation of 96 front end cards, and is a demonstration of what is needed to power the whole TPC. It also has feature such as a remote shutoff and status for remote operation.

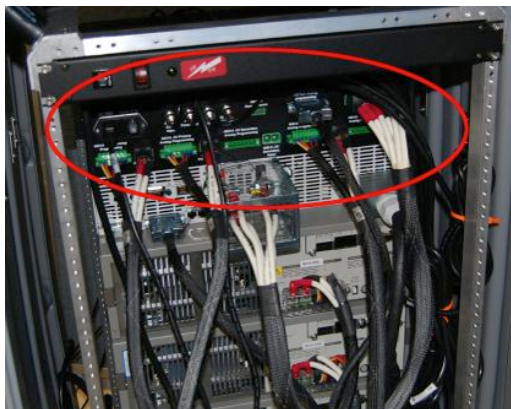


Figure 7: The power and clock distribution system.

Digital Bus Board

A production run of 30 digital bus boards was completed this quarter, and a full testing procedure has been developed. The boards will be tested this summer for the next run cycle.

Preamp Test Stand

The preamp card testing capabilities of the EtherDAQ GUI (GUI) have been greatly expanded. Previously, the GUI was used primarily as a method for controlling the pulse generator, as well as collecting the raw ADC data and dumping the data to a text file. The raw data was then externally analyzed using the ROOT framework. All the external analysis functions have now been incorporated into the GUI, thus providing a “one-stop shop” to provide all the tools necessary to analyze and characterize an EtherDAQ/preamp card pair. There are currently three tests: 1) burn-in, 2) linearity, and 3) cross-talk.

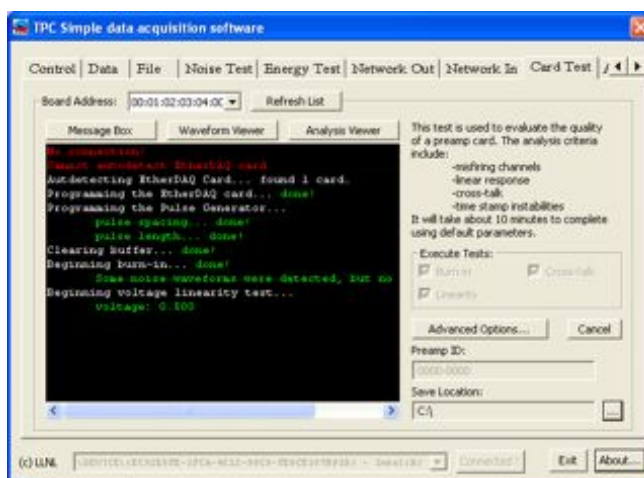


Figure 8. The EtherDAQ GUI in action with the burn-in test completed and the linearity test just beginning.

The burn-in test is used to pre-screen the EtherDAQ/preamp pair. All 32 preamp channels are enabled but the pulse generator is silent. All triggered data is collected by the GUI and analyzed. If a channel is determined to be noisy, i.e. generating false triggers, then that channel is internally masked by the software and the user is notified. If the number of noisy channels exceeds a predetermined limit then the test is halted and the user is informed that the EtherDAQ/preamp card pair is faulty. The card can then be shipped to LLNL for inspection.

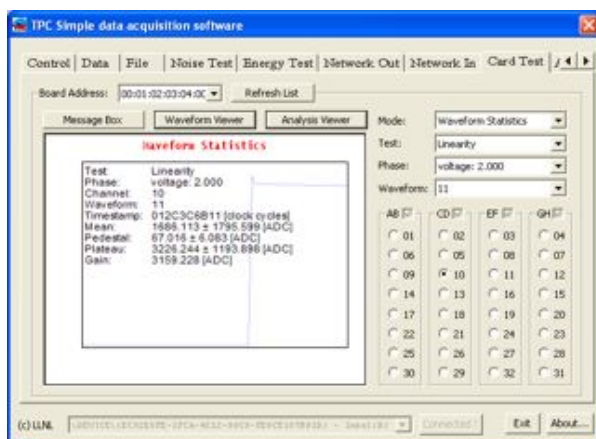


Figure 9. The statistics for each waveform can be inspected on an individual basis.

The linearity test routine analyzes the responses from each of the 32 channels. Primarily, the linearity analysis tests the response for each channel to ensure that the converted ADC values are proportional to the applied voltage. This is accomplished by sending pulses that cover a range of voltages. A linear regression is then fit to the gain as a function of the input voltage. The standard deviations from the gain calculations and the R2 value from the linear regression fit can be used as a metric of the quality of the response.

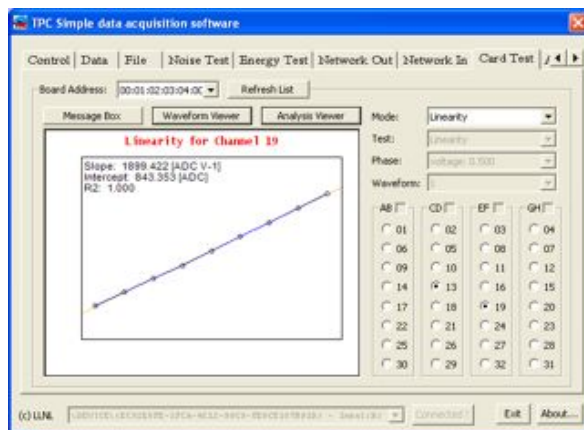


Figure 10. Results of the linearity calculations with corresponding linear fit.

Additionally, minor variances between the analog components introduce slight variations in the response amplitude between channels for the same input voltage. This is the case even though there are very tight tolerances for the components on the preamp card. The linearity portion of the test provides for a channel-by-channel calibration. The slope and intercept values from the linear regression fit can be stored in a database and later dynamically accessed to provide energy calibration for the actual TPC data analysis. This is especially important to enabling the <1% measurement error goal for the collaboration.

The final test is the cross-talk routine, which is still in development. Cross-talk cannot be neglected for the NIFFTE project because of the density of the electronics and proximity of the channels to each other. Essentially, cross talk occurs when a charge build-up in one channel causes a resulting charge to accumulate in neighboring channels. It is important to understand the magnitude of this charge sharing so that the effects can be accounted for and calibrated.

To analyze cross-talk contributions, an external trigger was created from the (t0) pulse of the pulse generator to enable a global readout of all channels coinciding in time with the leading edge of the first non-zero event pulse. By creating several sequential inputs, each with a leading pulse that corresponds to a different channel, the cross talk can be analyzed for all non-event channels. After discovering some timestamp anomalies, a new Etherdaq Card was obtained from LLNL that shows the expected timestamp even behavior. A copper Faraday Cage was constructed in order to reduce the observed noise (see Figure 11) when implementing the external trigger.

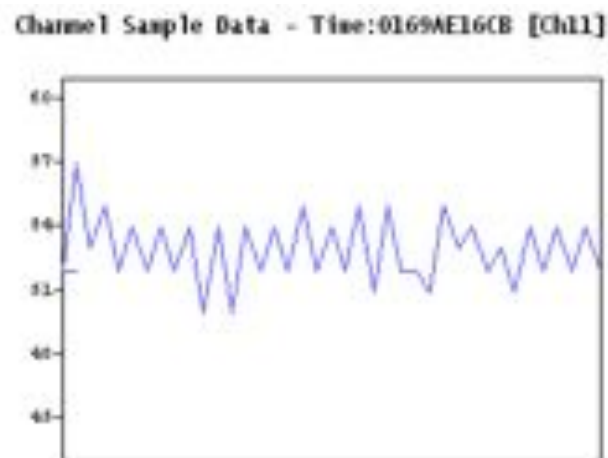


Figure 11. Noise in the pedestal of channel 11.

The GUI has been programmed with functionalities to:

- Visually display multiple waveforms simultaneously
- Zoom in on regions of interest
- Analyze timestamp consistency
- Analysis of pedestal values

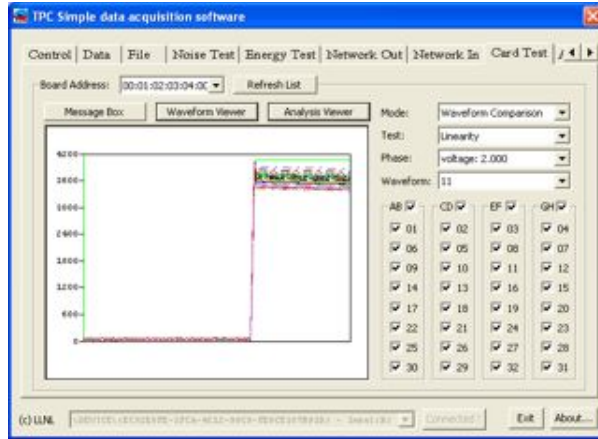


Figure 12. Waveforms from all 32 channels displayed simultaneously.

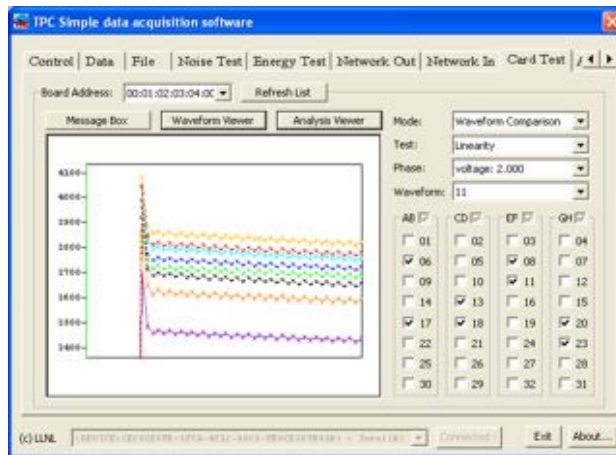


Figure 13. Zoomed-in view of a few randomly selected waveforms.

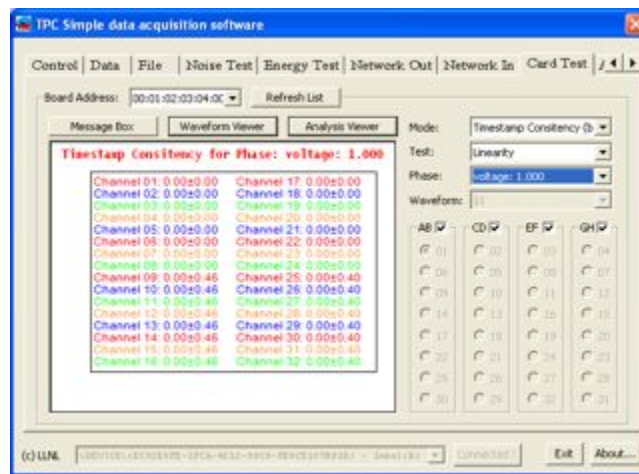


Figure 14. Timestamp analysis functionality.

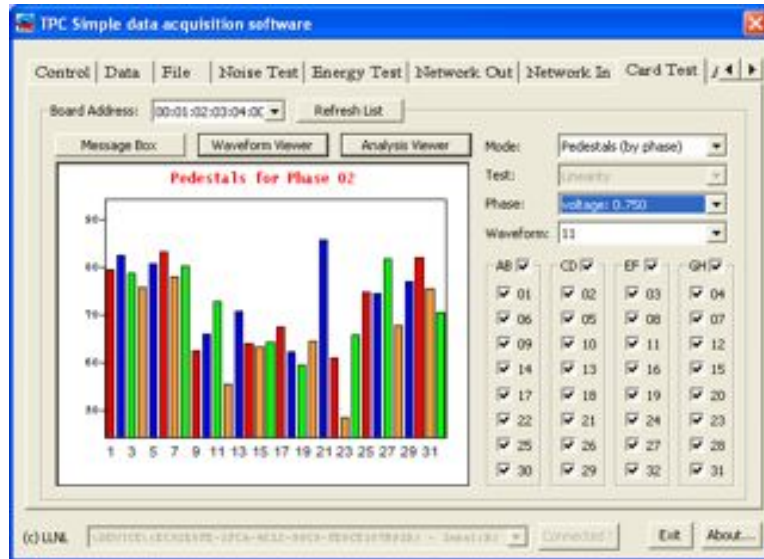


Figure 15. Pedestal analysis functionality.

Gas Handling and Temperature Control Systems [CSM, LLNL]

One dominant source of error in the absolute measurement of fission cross sections is the normalization of fission data to the U-235 standard. Any campaign that wants to improve on existing data will have to include a new absolute U-235 measurement. The U-235 reference is used to determine the total neutron beam flux, however this method incurs an error of no less than 1% due to the cross section error. The most promising alternative is the reaction $^1\text{H}(n,n)^1\text{H}$, which is known to 0.2%. This would though require the use of either pure Hydrogen or a very well known admixture as both target and detection gas in the TPC. In order to be not the limiting factor for the precision of the experiment, the hydrogen density will need to be known and kept constant within 0.1%. For calibration purposes, a gas admixture of Kr-83 will be used and in a later stage, one experimental possibility would be the use of a gaseous actinide target. We are planning for a system that allows for the use of three gases being mixed and supplied to the TPC.

Gas Supply System

The Colorado School of Mines group's main task in the NIFFTE collaboration is the maintenance and operation of the gas supply and control system. After the previous run cycle, the collaboration had requested that the general control of the system be migrated from the Windows to the Linux computer environment. This would enable the integration of the system into the same computing environment as the rest of the NIFFTE DAQ and slow controls. Additionally, it would provide the collaboration with remote control access to the system.

The migration to Linux required much of the proprietary hardware present in the old system to be replaced by relay boards. Much of the wiring from the previous gas system needed to be replaced. Taking advantage of the rebuilding opportunity, we also replaced the hardware enclosure to provide easier access to both the electronics and hardware elements.



Figure 16: The complete gas supply system hardware with relay board and power supply in the flight path.

The top of the enclosure contains the electronics control that consists of two relay boards. The Arduino Uno SMD is used to read out the status of the individual valves and transmits the information via USB to the NIFFTE gas system computer. The relay board, a ProXR RS-232 DPDT relay controller from National Control Devices, distributes the power to open the individual valves.

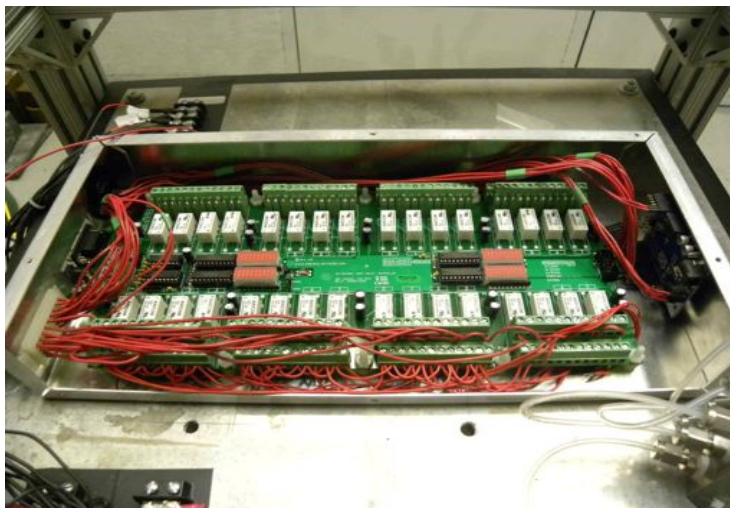


Figure 17: Relay board for solenoid valve control.

The relay boards are mounted directly above the pressure control hardware in order to keep the electronics wires as short as possible. This way, the complete setup only needs to be supplied with one ground connection, 5 V and 24 V from a common

power supply, pressurized air at 80 psi, one USB and one RS-232 computer connection.

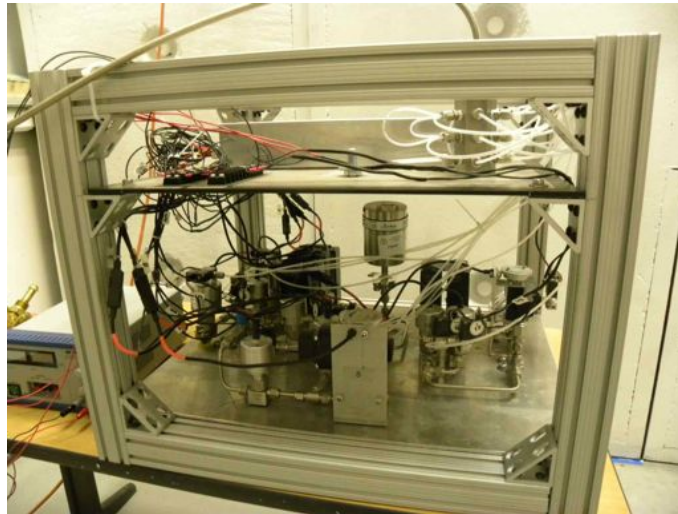


Figure 18: New gas system hardware enclosure for improved access.

As it appears that the measurement using radioactive target gasses is still a few years away, we decided to simplify the gas system hardware to the amount necessary for current measurements. This allowed more accessible placement of the elements in the same footprint as the previous system.

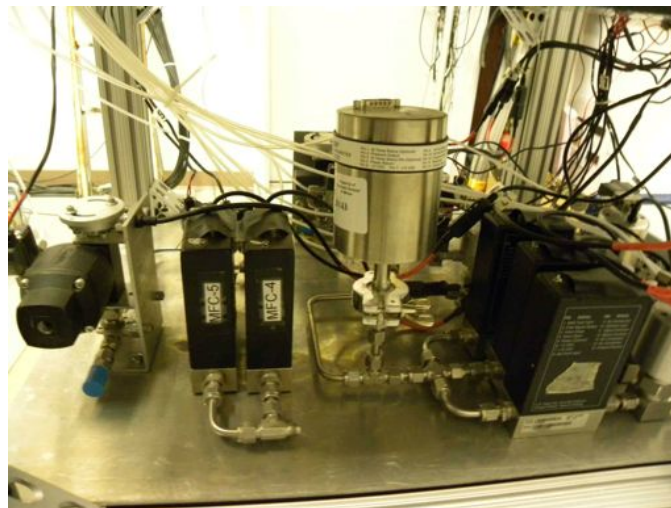


Figure 19: Close up view of the hardware components of the gas supply system as mounted in the new enclosure.

The valve control software is a C++ program and is completely operational. The gas flow and pressure monitoring is performed by MKS Instruments PR 4000 F and 647C

controllers. An open source program called Minicom is responsible for communication and control of these devices. In the coming weeks, we will integrate the system with the TPC and provide a pressure readout line to be included in the MIDAS experimental control system.

Electron Lifetime Monitor

The electron lifetime monitor is an important gas monitor to determine both the drift velocity of the electrons in the TPC as well as how much the gas impurities attach to the drifting electrons. In this quarter it was tested with P10 gas. Different algorithms were evaluated for the extraction of the relevant parameters (charge, lifetime, drift time, parallel diffusion constant). The cathode total photo-emitted charge was observed to drift over time. The reason for this behavior is being investigated. A PC-controlled oscilloscope was purchased and tested for use with the electron lifetime monitor. A custom C code was written to configure and control the scope. Operation on a Linux machine was also successfully verified. The analysis of the waveforms from the electron lifetime monitor was also improved. The use of Pockels cells and polarizers to reduce the pulse width of the Xe flash lamp was considered but then discarded due to the very poor transmittance of Pockels cells crystals in the VUV regime.



Figure 20: Shown here is the electron lifetime monitor vessel on the test bench at the LLNL TPC laboratory.

Target Design and Fabrication [OSU, INL]

A well-prepared set of targets is very important for high quality measurements of fission cross sections. Uncertainties in fission cross section measurements with fission chambers can be attributed, in part, to uncertainties in the target mass, non uniformities in the target, surface defects in the targets and surface contaminants in the targets, as well as impure target materials. While the proposed TPC for fission studies will allow detailed corrections for many of these problems, it is of great benefit to start with the highest quality actinide targets.

Target Design

We have established a proven ability to furnish targets of ^{238}U , ^{235}U , ^{232}Th and ^{239}Pu on both thick (540 $\mu\text{g}/\text{cm}^2$ or 81400 $\mu\text{g}/\text{cm}^2$ Al) and thin (80-100 $\mu\text{g}/\text{cm}^2$ C). We have shipped ~50 targets to the TPC collaboration. The targets we have furnished have been used to perform the initial testing of the TPC.

Now we are entering into a second phase of target development for the upcoming run cycle (CY12) in which the TPC collaboration will perform a number of critical measurements of the TPC. To make these tests, we will need a set of special targets designed to allow definitive testing of the TPC performance. These new targets, requiring unusual shapes of actinide deposits, variable thicknesses on a single target, the use of thin solid hydrogen containing targets and special deposit geometries to test the track reconstruction pointing accuracy were defined in an on-going dialog between us and the other members of the collaboration.

Some of the design issues that arose and their solution are as follows:

- (a) Design of the solid hydrogen target. Several materials were evaluated as solid hydrogen targets with polypropylene being chosen. This choice was made because of the relatively well-known composition of this material, the ability to get this material in appropriate thicknesses, and the lack of neutron absorbing materials (other than carbon and hydrogen) in the target. To prepare deposits of actinides on this material, we are using molecular plating on a polypropylene surface that is coated with about 2.4 $\mu\text{g}/\text{cm}^2$ Al.
- (b) Design of a ^{252}Cf "spot" target to test the track reconstruction pointing accuracy. This design effort is a work in progress with plans to produce these targets in two iterations, a simple "low resolution" spot target containing deposits of ^{252}Cf on 81400 $\mu\text{g}/\text{cm}^2$ Al prepared by evaporation, and a final "high resolution" version of the target prepared by molecular plating of ^{252}Cf on the same Al backing. Among the challenges that had to be solved were to obtain the ^{252}Cf material, to construct a special set of masks (see below) to define the high resolution spot patterns, to develop precise positioning devices for spotting the Al surface using automatic pipettors, the development of spreading agents to insure uniform evaporated deposits, the development of an appropriate surrogate for ^{252}Cf to test procedures, and to fabricate new plating cells for ^{252}Cf . Spreading agents being evaluated are a 5% solution of insulin in water and 2-(heptadecafluoro-decylsulfanyl)-ethylphosphonic acid. The latter compound will be synthesized using a radical chain reaction. [M. Essahi, et al., Journal of Fluorine Chemistry 127 (2006) 854.] As a surrogate for the ^{252}Cf in testing the procedures, we are using ^{153}Gd tracer ($t_{1/2} = 239.5$ d) prepared by activation of gadolinium nitrate in our TRIGA reactor. The masks for the "high resolution" molecular plating were machined from Delrin by Katon Precision Machining and involved hole patterns of 100 holes in a 9 x 9 mm square with hole sizes of 0.1 mm diameter. The "low resolution" targets are being spotted with 2 mm spacing between the spots on a grid of 10 x 10 mm with spot sizes of about 1 mm diameter.
- (c) Design of thin carbon targets with multiple coatings/thicknesses of ^{239}Pu on them in the form of wedges (see figures below). We have had a low success rate at putting four separate wedges of ^{239}Pu (by molecular plating) on 100 $\mu\text{g}/\text{cm}^2$ C. Even when we are successful in preparing the targets, we have observed them to dis-integrate spontaneously upon standing in air.

The "final" requested target designs are shown in the figures below.

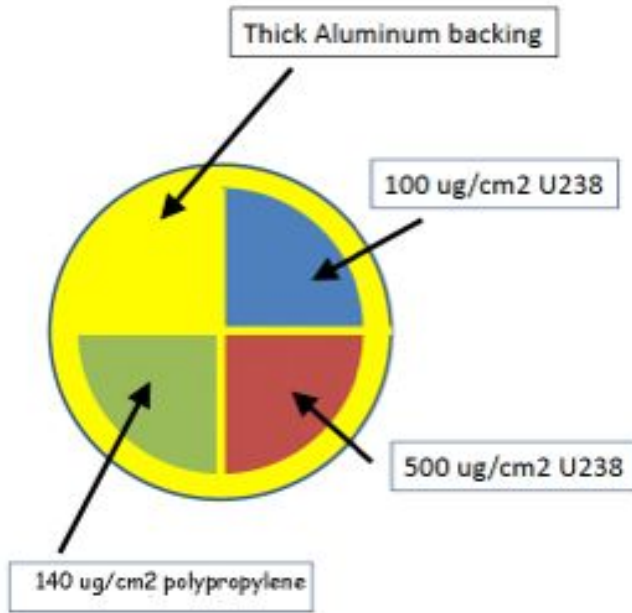


Figure 21: Front and back views of target CY12R0T0, The back side of the target is a uniform Pu-239 coating at 40 $\mu\text{g}/\text{cm}^2$.

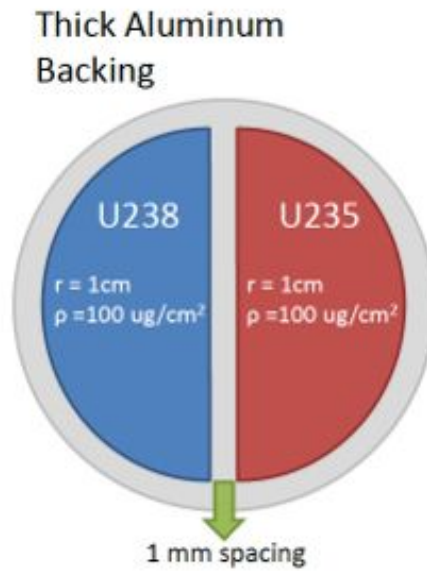


Figure 22: Design of target CY12R1T0.

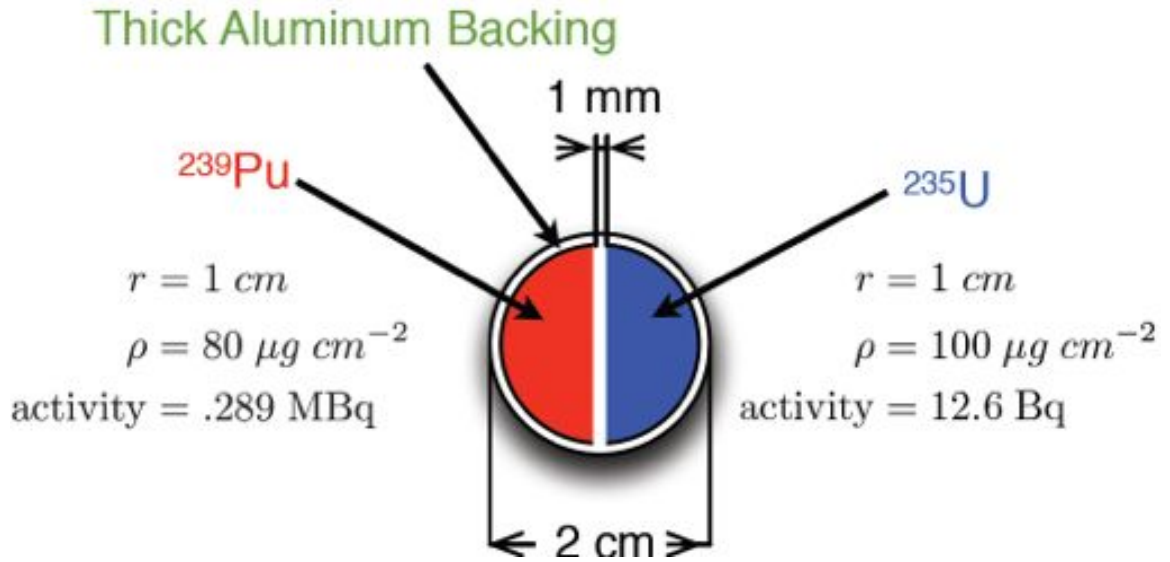


Figure 23: Design of target CY12R2T0.

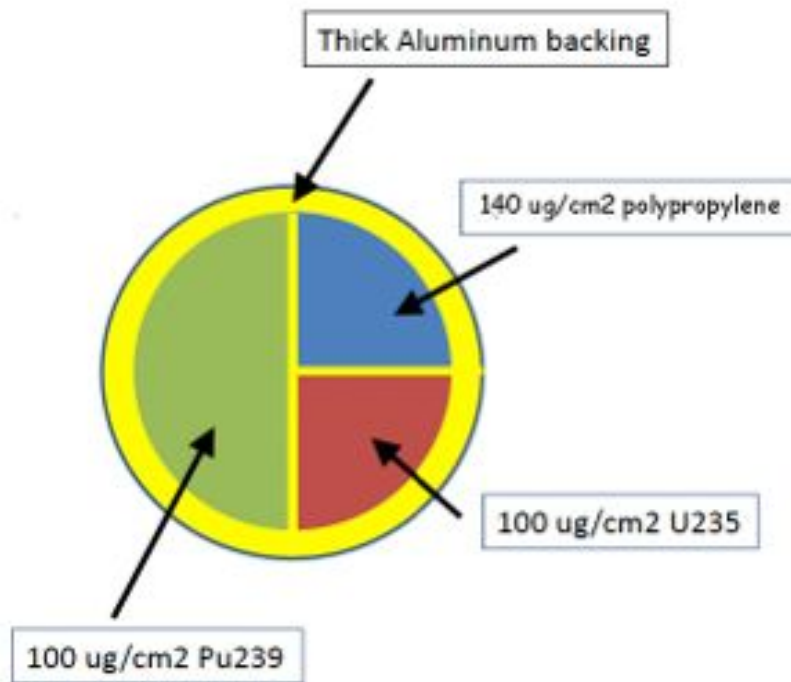


Figure 24: Design of target CY12R3T1.

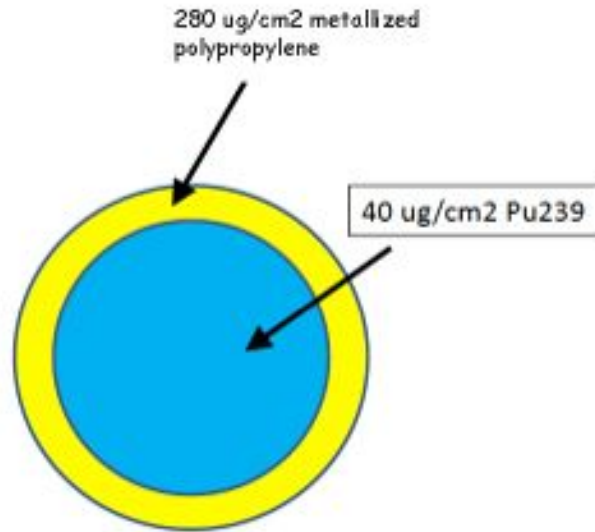


Figure 25: Design of target CY12R3T0.

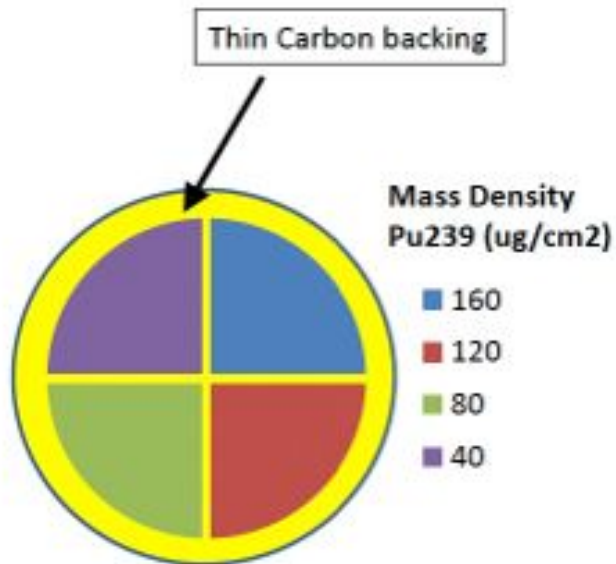


Figure 26: Initial design of target CY12R4T0. This design has not proven to be viable and modifications are being made—see text.

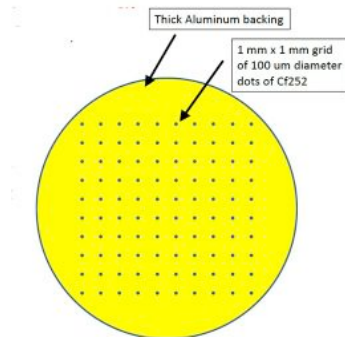


Figure 27: Front view of ^{252}Cf spot target design.

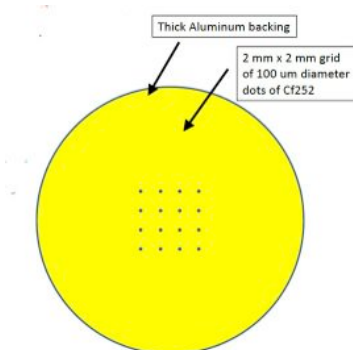


Figure 28: Back view of ^{252}Cf spot target design.

Target Fabrication

The following “target fabrication” activities were undertaken:

- (a) We hosted a group of three scientists from PNNL who are seeking to set up their own actinide target making facility. We provided demonstrations of preparation of ^{239}Pu targets by molecular plating and preparation of ^{232}Th targets by vacuum volatilization. We discussed several general issues in actinide target preparation. We prepared and shipped a test target to PNNL. The target designator was LY 5. The target consisted of half-circles of ^{238}U and ^{235}U of thickness 443 and 472 $\mu\text{g}/\text{cm}^2$.
- (b) We loaned a nominal 100 nCi ^{252}Cf source to LLNL for TPC testing.
- (c) We shipped a previously prepared ^6Li coated scintillator to ISU.
- (d) We worked on the re-design and alternate fabrication methods for targets CY12R4T0 and the ^{252}Cf spot target (see above).
- (e) In the process of assaying the various multi-isotope targets, we have noticed that the ^{239}Pu deposits “creep”, i.e., the activity moves outside the boundary of the deposit area. The transfer of material is very small ($\ll 0.01$ atom percent) and will not affect the use of the targets to measure cross sections. What this may affect is the use of the TPC to radiograph the targets because one will have to

distinguish the alpha decay of the low specific activity nuclides (^{235}U , ^{238}U) from the high specific activity ^{239}Pu .

Target preparation

The following targets were prepared and shipped to LANL:

TPC Target Designator	OSU Designator	Backing	Deposits
CY12R1T0	LY7	81400 ug/cm ² Al	302 ug/cm ² ^{238}U
			239 ug/cm ² ^{235}U
	LY 9	81400 ug/cm ² Al	122.5 ug/cm ² ^{238}U
			173 ug/cm ² ^{235}U
	LY 11	81400 ug/cm ² Al	115.3 ug/cm ² ^{238}U
			106.6 ug/cm ² ^{235}U
CY12R2T0	LY10	81400 ug/cm ² Al	105.1 ug/cm ² ^{239}Pu
			70.4 ug/cm ² ^{235}U
	LY12	81400 ug/cm ² Al	74.3 ug/cm ² ^{239}Pu
			63.9 ug/cm ² ^{235}U
CY12R0T0	LY6	81400 ug/cm ² Al	29.7 ug/cm ² ^{239}Pu
			456.9 ug/cm ² ^{238}U
			133.8 ug/cm ² ^{238}U
			140 ug/cm ² polypropylene
	LY14	81400 ug/cm ² Al	29.1 ug/cm ² ^{239}Pu
			954 ug/cm ² ^{238}U
			105.7 ug/cm ² ^{238}U
			140 ug/cm ² polypropylene
CY12R3T1	LY13	81400 ug/cm ² Al	112.4 ug/cm ² ^{235}U
			110.7 ug/cm ² ^{239}Pu
			140 ug/cm ² polypropylene
CY12R3T0	LY15	280 ug/cm ² polypropylene metalized with 2.4 ug/cm ² Al	25.3 ug/cm ² ^{239}Pu

TPC Software [CalPoly, ACU, ISU, INL]

Scope

The TPC Software effort will include online and offline coding, FPGA programming for the data acquisition system, and simulation. In addition to reconstruction and analysis of data acquired by the NIFFTE detector, the offline simulation and reconstruction software will be used to generate substantial "Mock Data Challenge" datasets of simulated fission events, alpha decays and background events that will be processed through the full simulation and reconstruction chain. In addition to testing the readiness and functionality of the offline software, these MDC efforts are intended to improve modeling and design of the actual NIFFTE detector.

Highlights

- A new 3D Hough transform track finding algorithm was implemented in the offline framework.
- Significant gains in offline processing have been identified through an analysis code profiling study.
- Work has begun to develop a refined tracking package with superior vertexing and particle identification that will be capable of extracting information for fission yields and charge configurations in the fission process.

Online Software [ACU]

The portion of this experiment's software library that is used during the data taking is called the online software. It overlaps in many ways with the data acquisition software, since it must take the data output from the readout cards after it has been processed with the FPGAs. The features that fall within the online category include: data receiver, event builder, data cataloging and storage, run control, on-the-fly data inspection, data base management, electronic log book, and remote experiment monitoring and control. Some of this software is available and only needs to be installed and maintained on the online computers, other software will have to be written and maintained in the collaboration subversion library. All written software will be written following a modular design for reusability in C++. In addition, the online software team will take on the role of administrator for the online computers.

Support for Operations at LANL

The online software has seen continuous development during the past quarter. Data collection at LANL was supported by installing, debugging, and maintaining the DAQ, slow controls, and online data quality assurance software. An important issue with the online demux performance was addressed. After analyzing some initial data with the TPC in the neutron beam, it was determined per-channel TPC trigger thresholds should be lowered to record significantly more recoil proton tracks from beam neutron interactions within the TPC.

Online Monitoring Maintenance and Development

The packet receiver and channel demux software were updated to handle waveforms from the HiSCaR. The event loop for the online channel demux software was modified to improve its data throughput capability.

The online event builder was modified and implemented to save a user controlled fraction of its output. For example, the program can save 100% of waveform events in when data rates are low or only 1% when rates are very high. This feature allows fine control over the amount of data passed to the CPU intensive online analysis and histogramming program.

MIDAS frontend program to store slow control measurements in the persistent SQL database has been updated to include recently added and modified channels. All the recorded variables are now saved with UNIX timestamp and the dates/minutes/seconds with time zone. This program was also modified to significantly reduce its CPU utilization.

Offline Software [CalPoly, ISU, INL, LLNL]

The thrust of this task is to transform the data from their raw form to final calibrated results, which requires a complete data analysis chain. The offline software required to perform this analysis must be designed, organized, written and documented. In order to achieve maximum flexibility, the design should focus on providing simple interfaces within a modular framework. For ease of use by collaborating experimenters, the software should also be well documented and maintained in a central repository available to the entire collaboration.

Analysis Code Profiling

During the analysis of raw data from the 2011-12 LANSCE run cycle, it was quickly identified that the analysis was taking a remarkably long time to complete, particularly for the Pu239 data. It was not immediately obvious which part of the analysis chain was causing this, or even if it was due to a particular module in the chain, so a code profiling effort was undertaken to better identify any critical bottlenecks or inefficiencies.

Valgrind (www.valgrind.org) is an open-source programming tool suite capable of identifying memory leaks, memory cache use, and call tree profiling, among other things. It accomplishes this by first converting the original binary executable into a processor-neutral intermediate form, which is then run on a virtual machine. The resulting execution speed is 20-100 times slower than the original, but the executable otherwise performs identically. Complete call tree and memory usage statistics are collected and reported during the execution.

The profiling was performed for the full production analysis chain for 1000 events from the U and Pu run. Some results are shown in Table 1 and Table 2.

Function	Percent of total execution time
NiffteRootIO::WriteEvent	40.8%
TPCHoughD::ProcessEvent	27.5%
TPCKalman::ProcessEvent	25.1%

Table 1. Percent of total execution time for selected functions in the NIFFTE production analysis chain, as reported by Valgrind.

The obvious conclusion is that writing the events to disk is taking a significant portion of the total analysis time. CalPoly collaborations quickly identified that NIFFTE data is stored in C standard template library arrays, but could instead be stored in ROOT TArrays, which would reduce the amount of data reformatting required when writing events to disk. Preliminary estimates of switching from STL arrays to TArrays in the NIFFTE analysis code implied a potential speedup of 2.8x; see the corresponding subsection for more details on that analysis.

Function	Percent of Hough execution time
ceil	5.6%
cos	31.2%
sin	30.2%
ResetHistogram	10.8%

Table 2. Percent of total execution time for selected functions in the NIFFTE production analysis chain, as reported by Valgrind.

Once the data storage format has been changed, the file I/O should drop to roughly 20% of the total execution time, and the optimization of the analysis code will become more important. Table Y demonstrates areas of potential improvement for the Hough track finder. In particular, standard library calls for sine and cosine trigonometric functions take over half of the processing time. Provided that the required resolution is achievable, replacing function calls with lookup tables could significantly speed this up. As another example, the ResetHistogram() function simply clears the contents of a histogram to zeroes, but the existing code was using an inefficient nested loop to do so.

Several easy optimizations are also present in the Kalman filter module. Improved code for the issues described above are being submitted for the next release of the analysis code, and Valgrind will be used to continue optimization of the NIFFTE production chain.

Track Reconstruction using the Combinatorial Hough method

The software profiling work identified the Hough subroutine as a place for some performance improvement. The Hough subroutine identifies hits in the TPC that fall

on the same line in 2D space. The Hough transform maps points in (X,Y) space to a polar coordinates space (ρ,θ) where lines are represented by angle and offset from the origin. The idea is that points that fall on the same line in (X,Y) space will map to the same point in the (ρ,θ) space. Searching the (ρ,θ) space for the most intense regions will give the points (digits in the TPC analysis language) that are all on the same line. Some minor inefficiencies in the search and initialization routines were identified and fixed. Those resulted in only minor performance improvements. The major inefficiency in the code is fundamental to the routine and involves filling the (ρ,θ) space with the family of lines that all go through the (X,Y) point. The number of lines allowed to pass through that point should be large for precision results but small for the routine to complete quickly. By definition, the vast majority of the looping will be for lines that are not representative of the data.

A potentially faster method is to use the Combinatorial Hough transform. Instead of cycling through hundreds of lines for each point, each pair of points in the collection of digits for a particular event is cycled through and the (ρ,θ) points representing the line between those points are recorded. Again, the most intense region of (ρ,θ) space then represents the line that encompasses the most points. This method will contain fewer iterations as long as the number of digits remains less than half of the number of lines tested in the original algorithm. For events with small numbers of digits, the Combinatorial Hough routine should be substantially faster.

A study was performed to test the performance improvement. The results for both track reconstruction routines were compared using the first 1000 events of a typical uranium target run (400000487) and the first 1000 events of a typical plutonium target run (400000838). The results of the study are shown in Table 3. The Combinatorial Hough method is certainly faster and the improvement is even more for the Pu data. Due to the large intrinsic activity of the plutonium, a higher detector threshold was used resulting in shorter stored tracks. These shorter tracks have fewer digits and so the percent improvement is larger for the Combinatorial Hough as would be expected given the two routines different dependencies on the number of digits mentioned above.

Table 3. Study of the time to convert from a raw file and perform track reconstruction for the first 1000 events using the original Hough and the Combinatorial Hough routines for the two different targets.

Target	Time to execute with Original Hough (s)	Time to execute with Combinatorial Hough (s)	Percent improvement
Uranium	9.17	7.65	17%
Plutonium	6.72	4.22	37%

An initial assessment of the performance of the Combinatorial Hough was completed. In some regions of the phase space there was good agreement between the original and Combinatorial routine while in other regions, there was less agreement. However, an examination of the tracking results for both algorithms reveals that neither is optimal yet. There are adjustments and optimizations that need to be made

to both algorithms to allow for more reliable track reconstruction. Examples of the necessary adjustments are the weighting method used for each event, the width of the tracks, and the coarseness of the (ρ, θ) space. Further study has begun using simulated data to compare the strengths and weaknesses of the two routines and hopefully lead to improvements in the algorithms. The initial particle conditions are better controlled in the simulation which allows the different algorithm behaviors to be examined in more detail.

Tracking Algorithms

A new 3D Hough transform track finding algorithm was implemented in the offline framework and is currently being debugged and tuned. Initial comparison between the new and old algorithm vs. Monte Carlo simulations indicate that we can expect some improvement in tracking accuracy once the new algorithm is optimized.

Offline Utilities and Data Processing

A web-based software to manage shifts for the LANSCE run was installed and configured, and an extensive shift page was setup for shifters. The shifts have been going well and we are getting good participation from folks to run the shifts around the clock.

New bug tracking system (TRAC) is installed and in use to track and prioritize both software and hardware related issues.

Automatic data transfers from LANL to LLNL are now in production mode. Run data is archived on tape within 2 hours of being taken.

Timing Offset Software Infrastructure Updates

Before the implementation of the High Speed Cathode Readout (HiSCaR) system in the TPC hardware, the z coordinate of an event was not well determined – all z coordinates were relative and calculated from the signal time (bucket number) recorded with the TPC waveforms. With the introduction of the HiSCaR precision timing signal, an absolute time reference ($t=0$) is established, so the absolute z coordinates can be determined. While implementing the changes required for the bucket number to z coordinate mapping, it became clear that it would be desirable to redesign the stored data objects so that the bucket number is stored and the z coordinate is always calculated. This allows for the possibility that post-processing can improve the HiSCaR calibration and modify the $t=0$ determination. The actual mapping between bucket number and z coordinate depends on a timing offset that must be determined for each event (and separately for each TPC volume as the triggers for each volume are independent).

The two plots in Figure 29 below demonstrate the implementation of the timing offset infrastructure. In the first plot, the z coordinates of the start of all reconstructed tracks are shown before any calculation of timing offsets. The distribution of start positions is due to diffusion near the start of the track. In the second plot, an artificial timing offset correction is applied which forces the vertex of each track to be at $z=0$. Although the HiSCaR timing offset algorithm is still under development, these plots demonstrate that the infrastructure is in place to manage the offsets once the algorithm is ready.

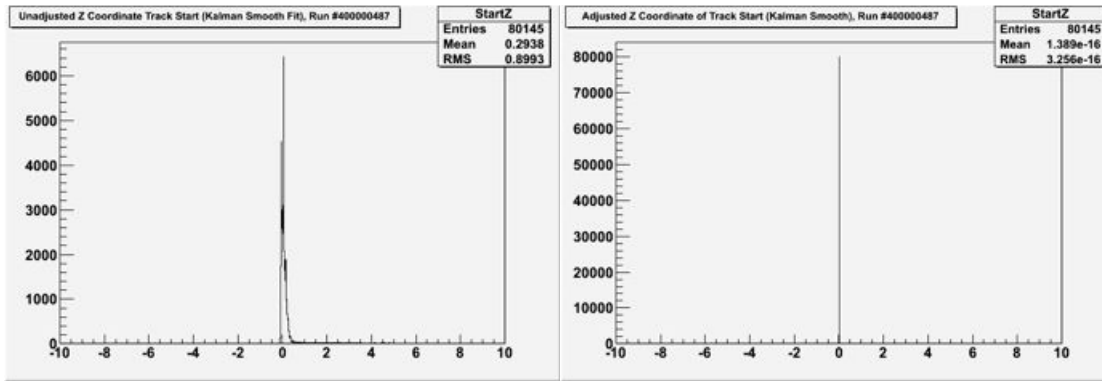


Figure 29: The z coordinates of the start of all tracks before and after the application of an artificial timing offset correction.

Hough Tracking Analysis

A visiting student at PNNL undertook an analysis of the Hough track finder. The existing Hough track finder relies on several input parameters, as listed in Table 4, and works reasonably well on data taken so far with the default values listed. However, a systematic study of the effects of varying these parameters has not yet been done, and the student who wrote the Hough tracking code is no longer available, so this is a worthwhile investigation. A PNNL report on the results of this study will be released next quarter.

Table 4. Hough track finder input parameters.

Parameter	Default Value	Description
WeighByADC	On	On = weight the digits by their ADC values Off = all digits weighted equally
DigitSharing	Off	Off = Each digit can only be assign to one track On = Allow digits to be shared between tracks
DigitThreshold	1	Digit ADC value must be above this to be considered for inclusion in a track
TrackThreshold	10	Minimum track ADC sum to be accepted as a track
HoughRadius	1.0	Expected radius of a track in the XY plane
HoughDiffusion	0.90	Expected radius of diffusion of a track

Refined Track Reconstruction

Work has begun to develop a refined tracking package with superior vertexing and particle identification that will be capable of extracting information for fission yields and charge configurations in the fission process. The proposed tracking package will include a fully informed global fitter that deconvolutes physical and detector-induced

distortions on the ADC signals, like electron diffusion and charge movements in the detector and the electronics.

The paradigm for the new fitter is to start the reconstruction process using tracklet hypotheses in the hexagonal voxels imposed by the geometric structure of the TPC anode plane. A fitter will refine and connect these tracklets to form a track instead of using points with an assumed a charge deposition occurring in the center of an anode pad.

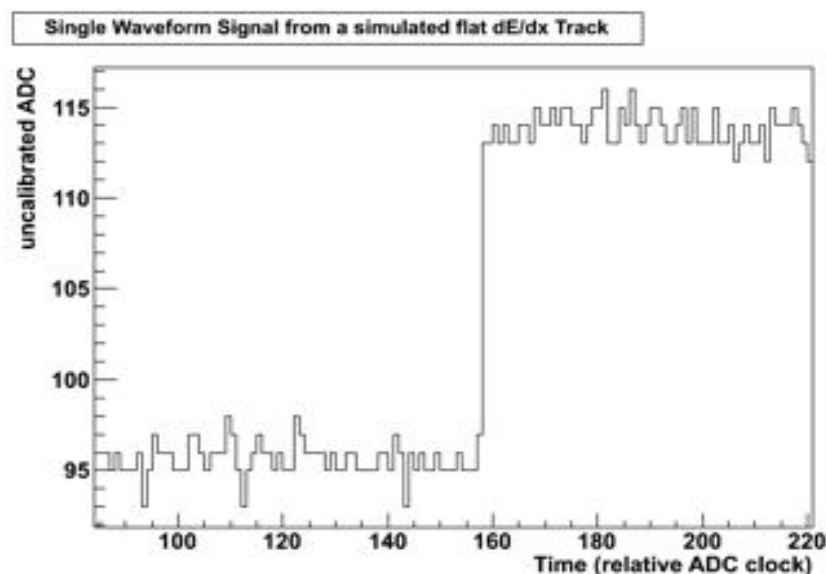


Figure 30: A single pad waveform signal in the shape of a step function from a simulated flat ionization loss track.

In order to learn more about the structure of the single waveform and to serve as a probe for any future tracking developments, the simulation package has been used to produce 'perfect' unperturbed waveform signals. For the particular task of testing and exploring waveform signals, the simulation was modified to produce signals from tracks that have a flat dE/dx profile (as opposed to ionization loss according to a Bragg-curve) and do not include any distorting effects like electron diffusion or charge distortion in the electronics. The obtained waveform is an almost perfect step function with a slight decay on the top of the rise due to the RC-constant in the electronics. Figure 30 shows an unperturbed signal from a track with flat ionization loss. This unperturbed waveform can be fit using a piecewise polynomial, while all three parts are a straight line with different slopes. The onset and edge of the rise can be found using a simple 7-point derivative filter. Due to the simplicity of the fit, it is actually possible to use an analytic least-squares fit using matrices, which increases the processing speed compared to a numerical fit.

When a more realistic ionization loss following a Bragg-curve is introduced into the simulation, the waveforms deviate from the idealized perfect step-functions. The edges of the rise become more curved and less pronounced, and the rise does not necessarily follow a straight line. A Fermi function coupled with an exponential RC-decay has proven to best fit those realistic signals.

The fit parameters of the signal waveforms are used to determine the impact of different distortions to the waveform by including them individually in the simulation.

Examples for distortions investigated are non-flat ionization loss, changing the RC decay constant and Preamp gain, diffusion in 3-dimensional space and a variety of charge distortions – charge sharing between neighboring pads or crosstalk between electronics. The goal of this effort is to deconvolute the distorting effects on the signal to be able to use unperturbed signals in the track reconstruction.

The radial information of the reconstructed track is pulled from the (x,y) coordinates of the anode pad for which the signal arrived. A well-informed tracking algorithm has to know the geometry of each hexagon, as the tracklets are made up by intersection points of the track with the hexagon structure rather than just the center of a hexagon. The (x,y) coordinates in the active volume of the TPC have been mapped to (row, column) coordinates uniquely identifying each pad on the anode. This enables the tracking software to extract an ADC signal from the corresponding pad from a certain (x,y) position. Recent efforts have led to a 3-dimensional mapping of the TPC by including a time bucket number in the mapping to produce 3-dimensional hexagonal prisms that make up the detector volume.

The initial (x,y) direction hypothesis of individual tracklets will be refined by forcing them to connect, and by tuning their length within a voxel based on polar angle and specific ionization.

Code execution time improvements

Potential improvements in code execution were identified in the analysis code profiling last quarter. Several of these were implemented this quarter in the Hough track finder and Kalman track fitter modules, resulting in minor speed improvements. In addition, updates to the persistent data objects, utilizing the fast I/O streamers built into the ROOT framework, were introduced. These changes yielded 70% improvement in the time to write reconstructed events to disk and a 30% improvement in the overall per event processing time. Several more significant code improvements are planned for next quarter.

Data Acquisition Software [ACU, LLNL]

This effort will develop all the software required to control the TPC experiment and log the data. An experiment control interface will be developed to allow collaborators to run and monitor the experiment from remote sites, including a slow control system with appropriate interfaces. The front-end cards for the TPC will be quite powerful and flexible because of the Field Programmable Gate Arrays (FPGA). The FPGAs do require programming which we will organize in a framework of modules (each module representing one task) for easy reconfiguration of the device. The modules that would be written for the FPGA would include (1) an ADC receiver that interfaces with the ADC chip, sending and receiving clock signals, receiving the serial data and presenting the data in a pipeline for the next module, (2) preprocessing modules would work with the data before zero suppression, and would include functions such as, ballistic deficit correction, fast proton timing, rebinning, and digital shaping.

Software Updates

The online software was used extensively during the WNR operation period by remote shifters and local operators. Monitoring for EtherDAQ status, TPC data rate,

and Ethernet traffic helped to identify several cases of degraded communication with multiple frontend DAQ cards. The hardware configuration change that coincided with these communication issues was reverted.

The overall data rate from the U238 and U235/U238 wedge combo targets is 200 kB/s with properly defined trigger threshold. The beam trigger mask was not completely deployed for this run cycle so the threshold was set very high to reject most of the alpha background in most of the Pu data runs. In this case, it turned out the data rate was at 700 kB/s as seen from Figure 31. Effort was taken to record data with low trigger thresholds for the Pu target as well to test the performance of the whole system chain. Thresholds are set up as 4up, 3 down for most of the channels while few noisy channels were configured with slightly higher thresholds. Figure 32 shows the reconstructed track length vs ADC from a part of a low threshold run. As expected, it appears that the most events are from alpha decay.

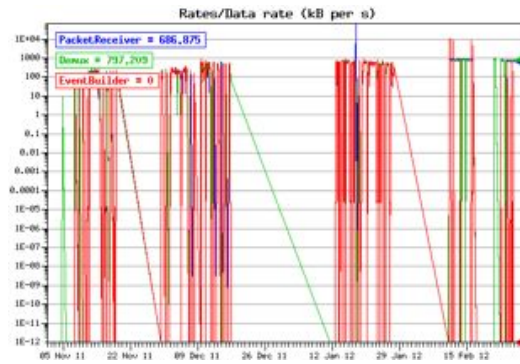


Figure 31: Shown here are the data rate monitoring for the run period.

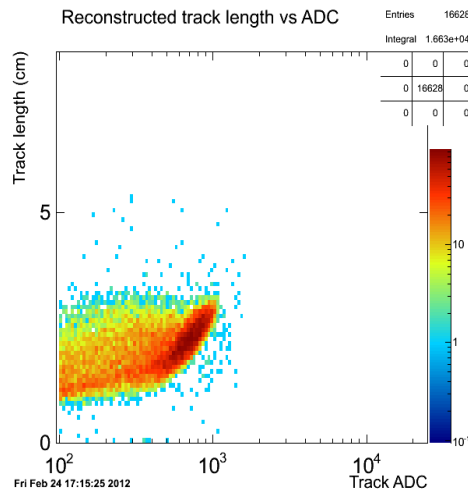


Figure 32: Shown here is the reconstructed track length with the ADC distribution from a portion of a low threshold Pu run from online monitoring. The run conditions were: pressure 972 torr, FCT/FCB/MMG -1200/-339/-340 V, average beam current 1730 nA, Lookback=65.

Simulation [CalPoly, ISU, LANL, PNNL]

Scope

In order to completely understand how the TPC will respond to various neutron environments and to accurately determine the fission parameters of uranium and the minor actinides, a complex simulation effort will be undertaken. The environments that the TPC will be used in will require accurate modeling of the detector systems used as well as the neutron production. MCNPX will be used to model the experimental setup at both the LANSCE, the quasi-monoenergetic neutron source at LLNL and Ohio University mono-energetic experimental facilities. These fully detailed four-dimensional models (3D space and time) will be used to create the source term for the GEANT4 modeling of the detector itself. Since MCNPX does not have the ability to transport heavy fission fragments, GEANT has been selected for this task. GEANT only has data for uranium fission events in the G4NDL library and the data for the remaining fissionable isotopes is based on a low precision neutron yield model. GEANT will need to be modified to use the Los Alamos model, also known as the Madland-Nix model, in which fission data will be added for U-238 and Pu-239 and the minor actinides. The modified GEANT module will allow the user to select the Los Alamos model or a fission distribution file supplied by the user. The fission fragmentation model will also be added to this module. To allow for a full model of the detector, another GEANT modification will be the addition of a static electric field modeling capability. This module will be used to accurately model the gas electron amplification inside the detector system. This will allow GEANT to completely model the detection system from birth (through MCNPX) to charge collection in the TPC pads. Using the high fidelity models of the experimental setup facilities, a series of databases will be created for various isotopes. This will allow for rapid comparison with experimental data.

Highlights

- Several improvements have been made to the GEANT4 geometry of the TPC in order to be able to simulate the different target designs that were proposed for the CY2012 run cycle.
- In an effort to better characterize the neutron source and neutron interactions in the TPC volume, including the scattering and room return effects, a new MCNP model of the 90L station and TPC volume is being developed.
- Detailed studies of the detector response continued in this quarter to understand the reconstructed ionization physical structure.

GARFIELD Simulations

As mentioned in the previous quarterly report, a particular type of track defect was identified for fission fragments, where a much slower data collection rate occurs for a subset of the charge. The hypothesis presented at that time was that the much larger number of electron-ion pairs being generated by fission fragments was resulting in a significant ion cloud in the region of the track, which was affecting the drifting electrons. An example from actual data is shown in Figure 33.

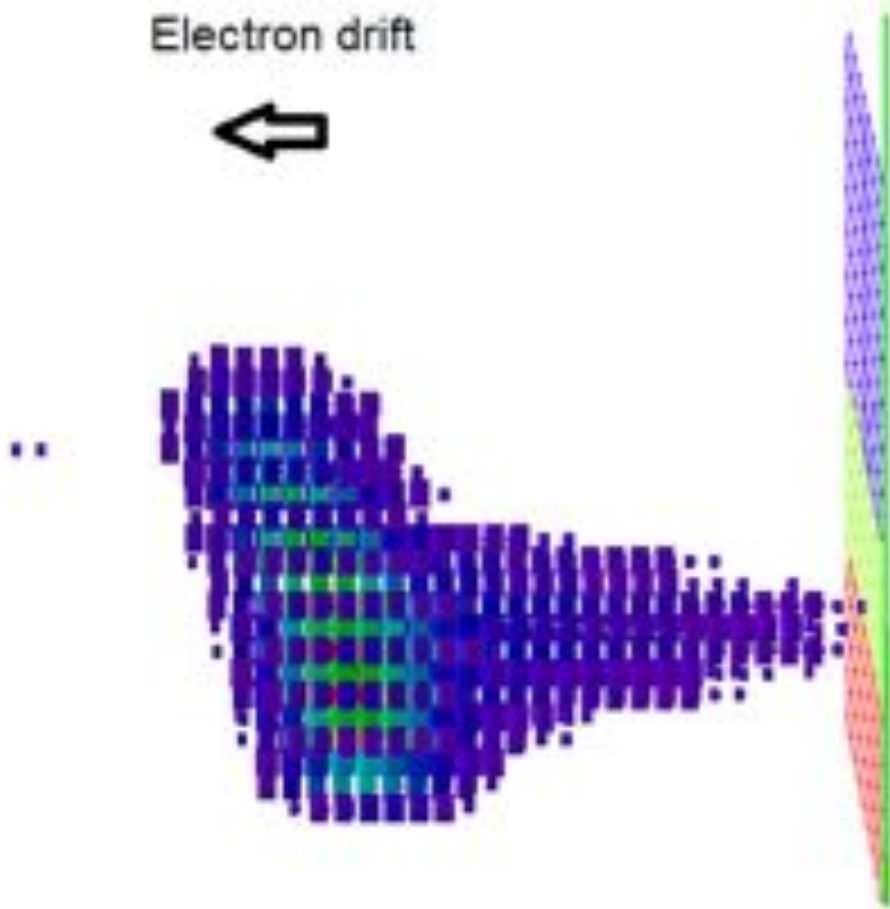


Figure 33. Example of the delayed drift time effect in actual data (electron drift and collection occurs to the left). The “tail” of charge to the right of the track actually represents electrons arriving later than expected. The track has incorrectly identified it as a separate track.

To better study this, a simple GARFIELD simulation was run, with the simple geometry of two 8 cm x 8 cm plates with voltages of 0V and -840V placed 5.5 cm apart representing the TPC. Provided that the drifting electrons stayed near the center of the plates, then the lack of field cage had only a minor effect on the simulation. To get around limitations of GARFIELD, which assumes that all defined shapes are solids and thus block electron drift, an electric field was calculated with an external tool and imported into GARFIELD. The finite element analysis tool Maxwell was available and used for this effort.

With Maxwell, cylindrical charge clouds of radii from 10um out to 100um were generated horizontally, and electrons drifted from a line below and perpendicular to the cloud drifted past (and through) it. If the hypothesis was correct, then electrons that drift through the cloud should show longer drift times than those that drift some distance from it. Figure 34 shows results for radii of 10um, 25um, and 100um.

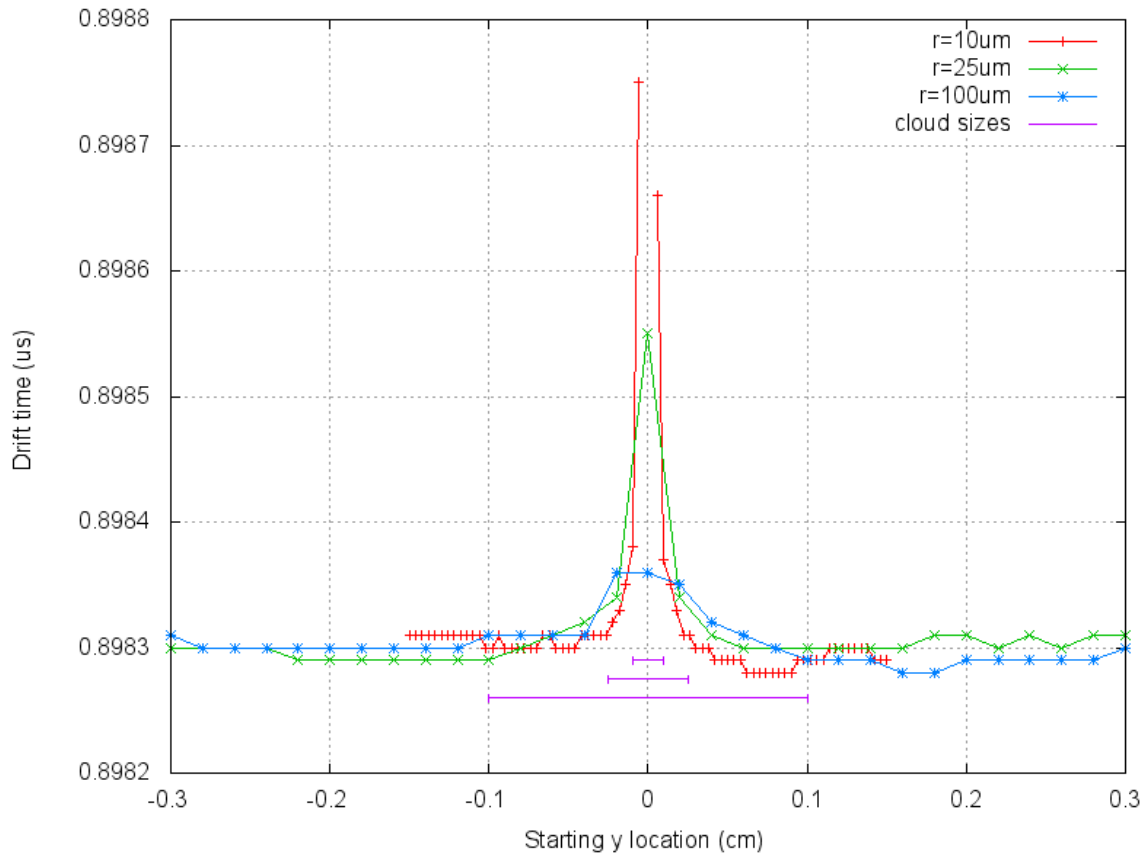


Figure 34. Calculated drift times for electrons drifting

While it can be seen that electrons that pass through the charge clouds have longer drift times, and the drift times increase as the charge cloud radii decreases, the effect is only about 1/1000 as large as has been identified in the actual data.

Investigation of the parameters used in these simulations is underway to identify any potential errors in the analysis. In addition, analytical estimates of the effect are now being undertaken to confirm the magnitude of the effect as seen in simulation.

Improvements to Particle Transport and Event Generation inside Geant4

Several improvements have been made to the GEANT4 geometry of the TPC in order to be able to simulate the different target designs that were proposed for the CY2012 run cycle. These improvements include the ability to insert different sections of the source to simulate the wedges or separate circles (see Figure 35). Other improvements include how the position of the event is chosen.

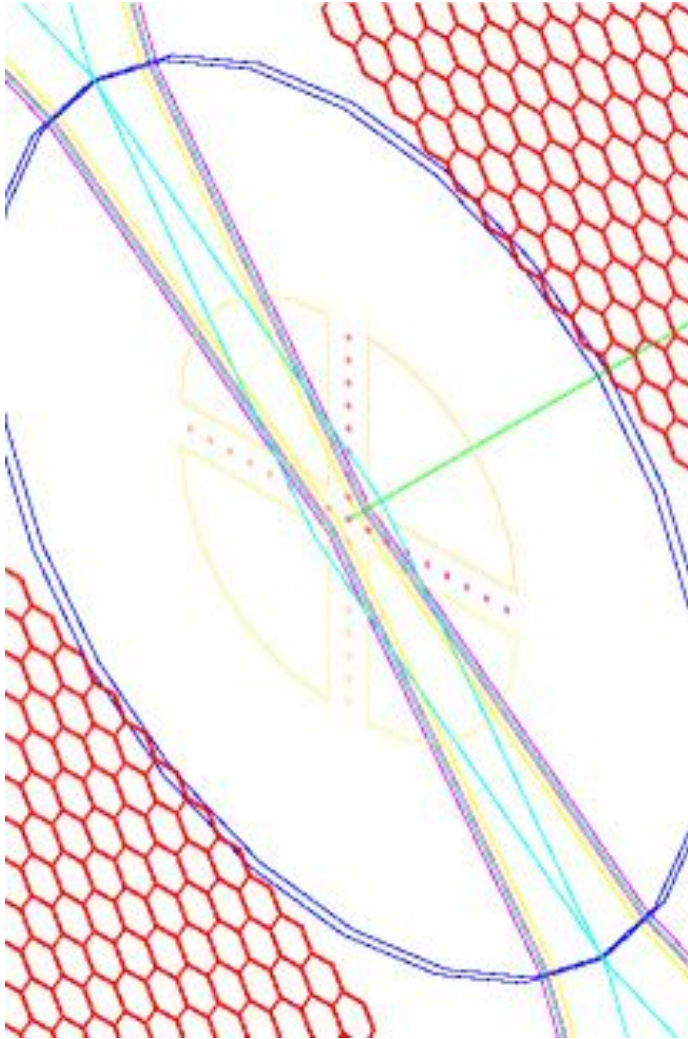


Figure 35. Source material shown in Geant4 as a cross and four wedges.

The initial positioning part of the event generation is now running inside of Geant4 as an independent module, and the user has the ability when running Geant4 to choose which method should dictate the starting location of the event. The methods include “fixed”, “uniform”, “uniform based off source intensity”, and “histogram”. Uniform based off source intensity chooses the source insert according to the intensity and then uniformly chooses the start position inside that insert.

Similar improvements have been made to the G4FissionFragmentGenerator where only a fixed neutron energy was available. The user now has the ability to choose between a fixed, uniform between given range, absolute Gaussian, user defined histogram, and published spectrum for LANCE-WNR 90L beam. The details of the incident neutron are now also saved in the output data file as an MCParticle.

In addition, the user can now turn off multiple scattering while running Geant4. This was added to test how the reconstruction changes with and without multiple scattering.

Kapton dielectric, electric field, and the pressure vessel were added to the default geometry, to better simulate what happens when a particle interacts with the edge of the active volume.

Improvements to Detector Response Simulations

In order to better understand the results coming from the TPC, two cross talk modules have been created for the detector response simulations. One module is to simulate the cross talk between traces on the pad plane and the other to simulate the cross talk between traces on the preamplifier card. Each module at the moment assumes a uniform percentage of charge shared to all nearest neighbors for every trace.

To be able to test out a new track fitter, a module to normalize the dEdx for one track events was added to the detector response simulations. The module will only work for one track events using a hexagonal geometry. Full tests of the module are currently ongoing.

MCNP Simulation of the Fission Ionization Chamber

In an effort to better characterize the neutron source and neutron interactions in the TPC volume, including the scattering and room return effects, a new MCNP model of the 90L station and TPC volume is being developed (see Figure 36). The basic MCNP geometric model of the area is based on recent measurements and photographs, and will be benchmarked against published data from a standard fission chamber (Figure 37) used in that location. A realistic TPC volume will then be added to the MCNP model.

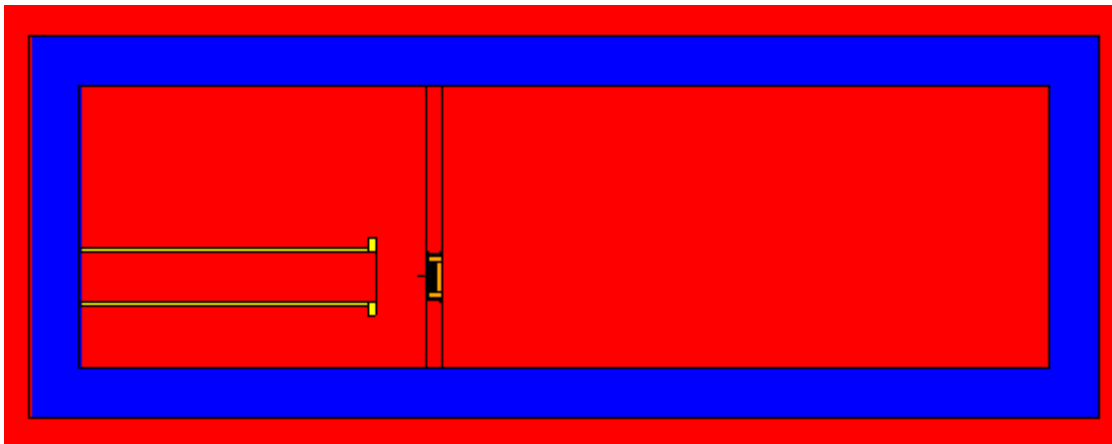


Figure 36. A side view of the MCNP model of the 90L station. Each individual color represents a particular material.



Figure 37. An updated cross-sectional view of the representative fission ionization chamber.

Delayed charge analysis

Last quarter, GARFIELD simulations were run to identify whether the ion cloud left by a fission fragment traversing the TPC was potentially the cause of the “delayed charge” effect seen on fission fragment tracks, where a small portion of the charge was collected much later than the rest of the track (see Figure 38). The hypothesis was that electrons that had to drift through the ion cloud were being delayed by the effects of the ion cloud on the local electric field. The preliminary simulation results indicated that a delaying effect was occurring and that the effect was greater for narrower ion clouds, but that the magnitude was about three orders of magnitude too small to match what was seen in the TPC data. The results were rechecked for accuracy and confirmed.

Secondary electron emission from the cathode plane (or target itself) was investigated as a possible source of the delayed charge as well. As a highly-charged fission fragment traverses a metal, it generates secondary electrons due to both Coulomb interactions with atomic electrons as well as knock-on electron generation. At depths in the metal below about 10^{-7} cm, the electrons tend to recombine in the metal, but near the surface these electrons can escape (Sternglass, 1957). Measurements of secondary electron emission from UO_2 metal have been shown to produce hundreds of electrons per fission fragment, depending on the metal thickness (Anno, May 1962), so the number of electrons is sufficient to potentially provide a signal in the TPC.

Whether the geometry of secondary electron emission matches the signal is currently under investigation; the interplay between the depth of the interaction in the metal and the dE/dx deposited per unit length makes it unclear whether the observed delayed charge matches the expected distribution.

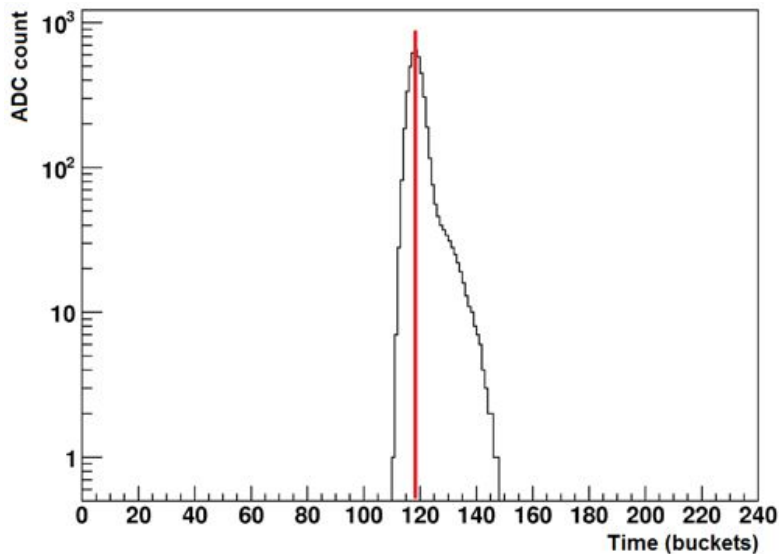


Figure 38. ADC count vs. time for a single channel. The red line represents the mean value of a gaussian centered on the charge from the primary track. The delayed charge cloud is evident in the additional counts to the right, signifying a later arrival time.

It was identified that the ability to automatically select events with the delayed charge was necessary, and so the track geometry of those events was investigated. The presence of two tracks in the event was required as a simple method of selecting events of interest, since the tracker frequently fit the delayed charge tail with a track; plotting the total ADC against the number of tracks per event (see Figure 39) demonstrates that 2-track events are more likely to have higher ADC values and hence contain a fission fragment. On top of that selection criteria, an azimuthal angle cut on the primary track of greater than either 45° or 80° was added to identify any dependence on primary track angle.

It should be noted that the track's azimuthal angle has several obvious effects on the identification of the delayed charge cloud as a secondary track. First, if we assume that the delayed charge cloud always points back to the cathode plane (which is what is observed), then the tracks will tend to combine primary tracks with low azimuthal angles with any potential delayed charge cloud, since they essentially lay on top of each other. Second, primary tracks with azimuthal angles of $30\text{-}45^\circ$ tend to "steal" charge from any delayed charge cloud, essentially bending the charge cloud's track identification in the same direction as the primary track. Only at larger angles such as 80° , where the delayed charge is at nearly right angles to the primary track, is this effect minimized.

Preliminary results from this track geometry analysis show that it is possible to select delayed charge events with these simple cuts, but only if the tracker identifies the delayed charge as a separate track. The study will continue in the next quarter to better assess event selection to include events where the delayed charge is not so obvious.

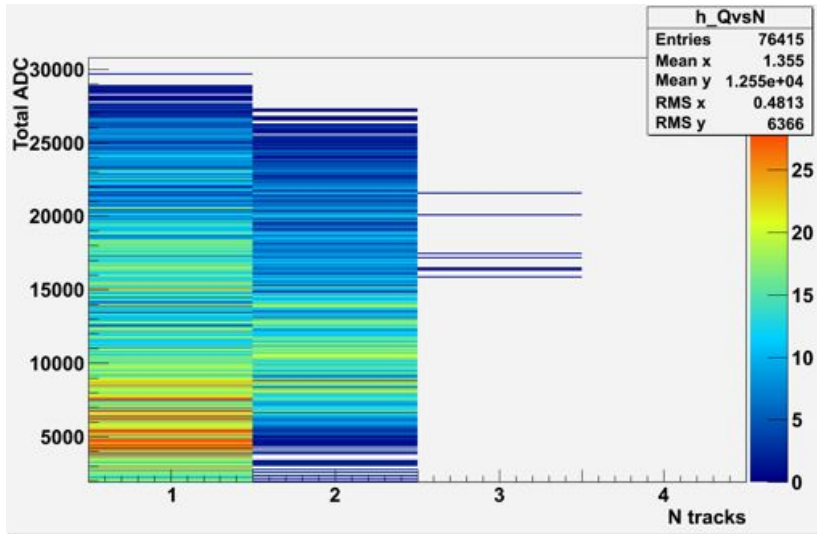


Figure 39. Total ADC vs. number of tracks per event. There is a clear indication that 2-track events have greater ADC values, implying that they are more likely to contain a fission fragment.

In an attempt to better understand the cause of the delayed charge effect, the channel ADC data (such as in Figure 39) was examined in more detail for events exhibiting the effect. The signals for each channel were fitted with a Gaussian shape, and the ADC count outside that peak due to the delayed charge was plotted versus the area of the fitted signal pulse (i.e. total ADC counts). Preliminary results appear to indicate that events with larger pulse heights have a higher likelihood of having a delayed charge tail, but some events with large amounts of charge have no charge tail. Also, the fraction of the charge in the tail to the total does not remain constant, but leads to a range of pulse shapes. The location and direction of the tracks is being examined for correlations with events with delayed charge.

Data Analyses [CSM, LANL, CalPoly, ISU]

Scope

The TPC data is analyzed early in the program to validate operation and design choices. The early analyses include data collected using partially instrumented instruments, using sources and neutron beams, including the proto-type TPC as well as the production versions. These analyses are used to test the complete system and to determine the overall quality of the data through the complete hardware and software chain.

Highlights

- Working toward the goal of developing robust particle tracking and identification capabilities, a partially instrumented TPC was used to measure the alpha/SF branching ratio in Cf-252. An initial analysis of the Cf-252 data is complete and the branching ratio was measured to within 1% of the accepted value.
- The particle ionization characteristic from both Pu and Uranium data has been studied to better understand the detector performance, such as the space charge effect from the track density inside the TPC gas volume.

Cf-252 Alpha Decay to Spontaneous Fission Branching Ratio

Working toward the goal of developing robust particle tracking and identification capabilities, the fission TPC is being used to measure the alpha/SF branching ratio in Cf-252. An initial analysis of the Cf-252 data is complete and the branching ratio was measured to within 1% of the accepted value. The measurement of alpha/SF was completed with 1 sextant of the TPC instrumented, or 1/12th of the total detector, and a 100 nCi Cf-252 source mounted on a platinum backing. This is a challenging exercise as the limited fiducial coverage leads to effects that constitute the major contributors to the overall systematic errors in this particular study. A fully instrumented TPC will not suffer from these limitations.

The source composition was determined by measuring the alpha decay spectrum of the source with a silicon diode detector. The alpha and fission spectrum of the Cf-252 button source as measured by the silicon diode detector can be seen in Figure 40. The source activity was determined to be approximately 97.3% Cf-252 at the time of the measurement. The alpha/SF branching ratio was also extracted from this data and was found to be within 1% of the accepted value.

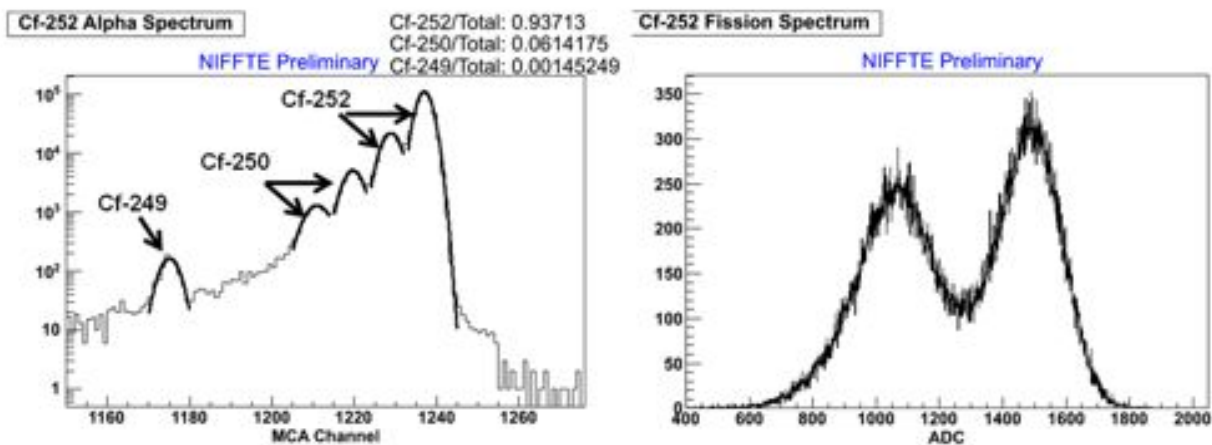


Figure 40: The alpha spectrum of the Cf-252 button source as measured with a silicon diode detector. The plot on the left shows the alpha spectrum, the y-axis is in logarithmic scale. The plot on the right is the fission spectrum. The expected major contaminates were Cf-249 with an alpha energy of 5.813 MeV (82.2%) and Cf-250 with alpha energies of 6.030 MeV and 5.989 MeV (84.6% and 15.1% respectively). The expected alpha energies from Cf-252 are 6.118 MeV and 6.075 MeV (84.2% and 15.7% respectively). These five peaks are fit with Gaussian functions. The ratios shown on the top right the alpha spectrum plot is the area under the associated peaks divided by the total of all the peak areas.

SRIM simulations and published data were used to account for the effects of the scattering of alpha particles and fission fragments in the source. The Cf-252 source was mounted on a thick platinum backing and covered by approximately $100 \mu\text{g}/\text{cm}^2$ of gold. In principle the available solid angle for emission from the sources is 2π , however it is not expected that the detection efficiency will be 50% due to the effects of scattering in the source backing and cover. Alpha particles (and in the case of the Cf-252 source, fission fragments) incident upon a metal backing will occasionally scatter through a large angle due to an interaction with a nucleus (Rutherford scattering), and be emitted from the surface of the source and into the active area of the detector. Even more often than Rutherford scattering, an ion will undergo multiple scattering at small angles with the atomic electrons, the cumulative effects of which can result in backscattering, particularly if the initial trajectory of the ion was at a grazing angle with the surface of the metal backing. In this context then, backscattered refers to an ion with an initial velocity vector towards a surface which then scatters and is left with a velocity vector away from the surface, not necessarily an ion that is scattered through an angle greater than 90 degrees. Figure 41 shows the polar angle distribution of alpha particles from a TRIM simulation of a 4π alpha point source mounted on a thick platinum backing and covered by a thin gold foil, also shown is the data from the TPC. The active volume of the TPC was defined to be between a polar angle of 90-180 degrees, where the polar angle is the angle with the axis that is perpendicular to the plane of the source. An ideal point source would then be expected to have a flat distribution of tracks as a function of the cosine of the polar angle. The simulation and the data both show a predominance of tracks near a cosine of zero, which is near parallel with the surface of the source. This is a result of alphas that have backscattered in the platinum backing and then been transmitted through the active, gold covered side of the source.

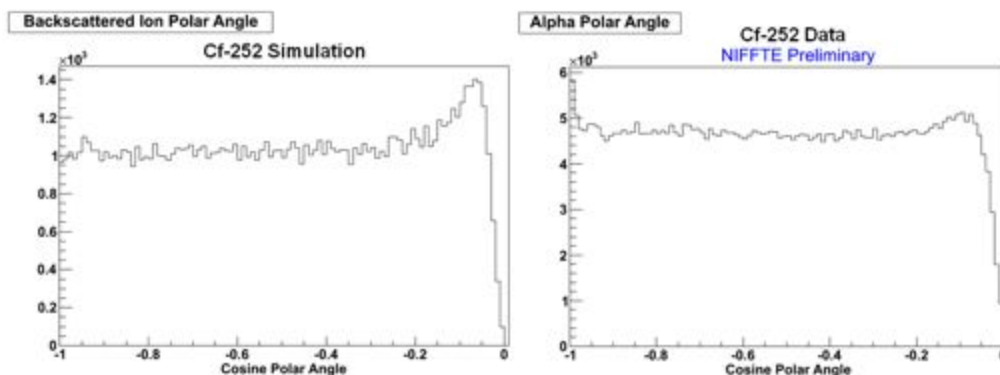


Figure 41: The left plot is a simulation of the Polar angle distribution of the alpha particles that have either been transmitted directly through a $100 \mu\text{g}/\text{cm}^2$ gold covering or backscattered off a thick platinum backing and then transmitted through the thin gold covering. The simulation was based on a 4π point source of 6.118 MeV alpha particles positioned between the gold covering and platinum backing. Note the peak in the count rate near cosine equal to zero, which is a result of excess particle tracks from backscattering. The Plot on the right is the polar angle distribution of alpha tracks in the TPC. A similar peak in the count rate near cosine equal to zero to the one in the simulation is exhibited. The polar angle is defined as the angle with the axis that is perpendicular to the surface of the source. Cosine equal to zero then is parallel to the surface of the source.

Figure 42 shows the length vs. ADC of fission fragment and alpha particles in the TPC. Graphical cuts show the number of alpha particles and fission fragments and the ratio of the two numbers. The branching ratio shown in the graph must be multiplied by a factor 2 to account for the fact that with a 2π source there are at least two chances to detect every fission event. Doing so will give a ratio of approximately 33.36 which is higher than the expected value of 31.34. The ratio has not been corrected for backscattering however. Due to the high nuclear charge of fission fragments, they are generally more susceptible to backscattering than alpha particles resulting in the ratio being higher than expected. The details of a backscattering correction will not be discussed here, but after applying a preliminary correction a ratio of approximately 31.08 – 31.19 is calculated (the exact value depends on the details of the application of the backscattering correction). While this value is preliminary, it is within 1% of the accepted value of the alpha/SF branching ratio of Cf-252. Considering the limitations imposed by having a partial detector and the use of a non-optimum source (i.e. the thick platinum backing which causes backscattering), the results are quite good and go far in confirming the abilities of the fission TPC to track, identify and distinguish alpha particles from fission fragments.

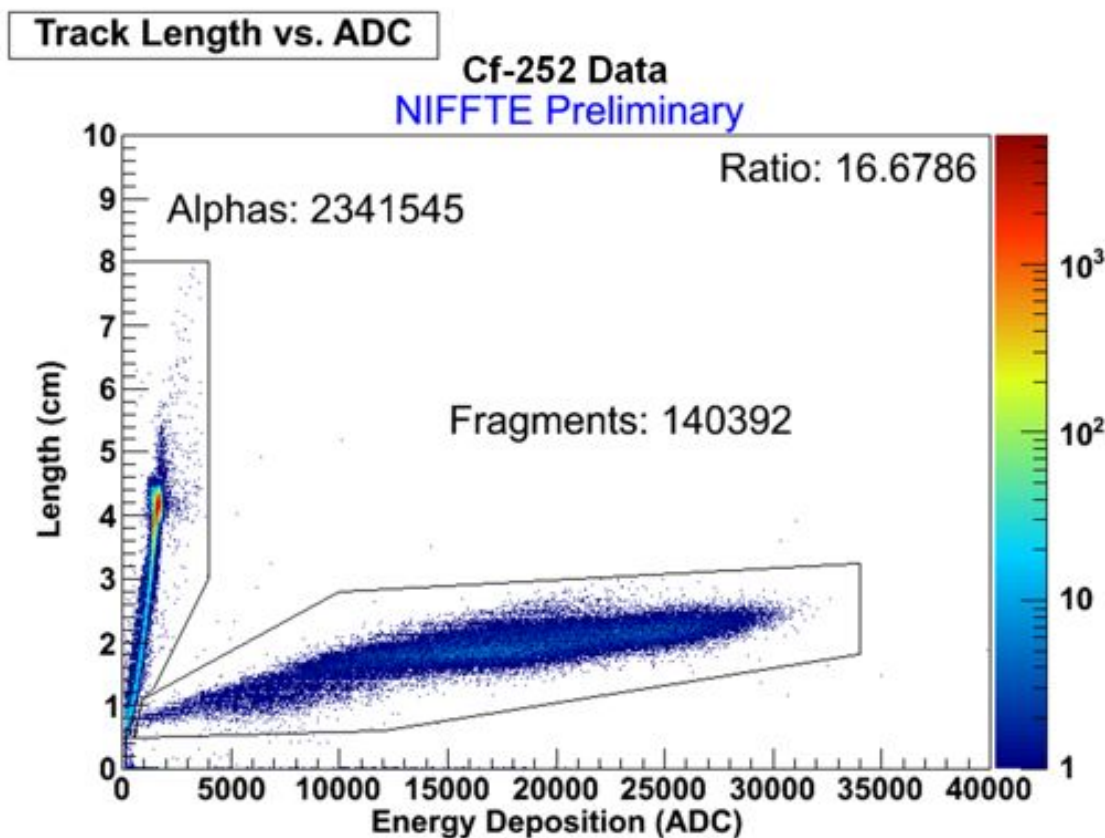


Figure 42: The track length vs. the ADC of particle tracks in the TPC. The color scale is logarithmic. The band on the left at low energy with long track lengths are alpha particles, while the high energy short tracks are fission fragments. The number of fission fragments and alpha particles are based on the graphical cuts drawn. The tracks were between 35 - 85 degrees azimuth and 90 to 180 degrees polar.

Luke Snyder from the Colorado School of Mines defended his PhD thesis successfully in March based on the first data from the one segment (1/12) operation of the NIFFTE TPC. His thesis describes an analysis of the alpha to spontaneous decay channel ratio in the nucleus 252-Cf. His results are compatible within error (experiment achieved competitive precision) with previous measurements. Additionally, due to the tracking capabilities of the TPC it was possible for the first time to directly measure the fraction of back-scattered particles originating from the platinum source backing. Given the complex geometry of the partial detector the analysis was very successful and provided an excellent start to the physics program of NIFFTE.

WNR Data Collection

There are total 950 runs (846 physics runs) of data collected with raw pcap data file size of 2.18TB (2,183,313,959,341 Bytes). Figure 43 shows the run number versus the raw data file size. At the end of the run cycle, effort was taken to collect the Pu beam data with low threshold. It turned out the data rate went up to ~100MB/s. Few short runs with low threshold were successfully taken with 25GB in about 5 minutes each. The average beam current is in about between 1500 and 1700 nA and is stable during operation period (Shown in Figure 44). The performance of TPC electronics shows very stable and calm, the warmest card temperature recorded was never above 38 degree (Shown in Figure 45).

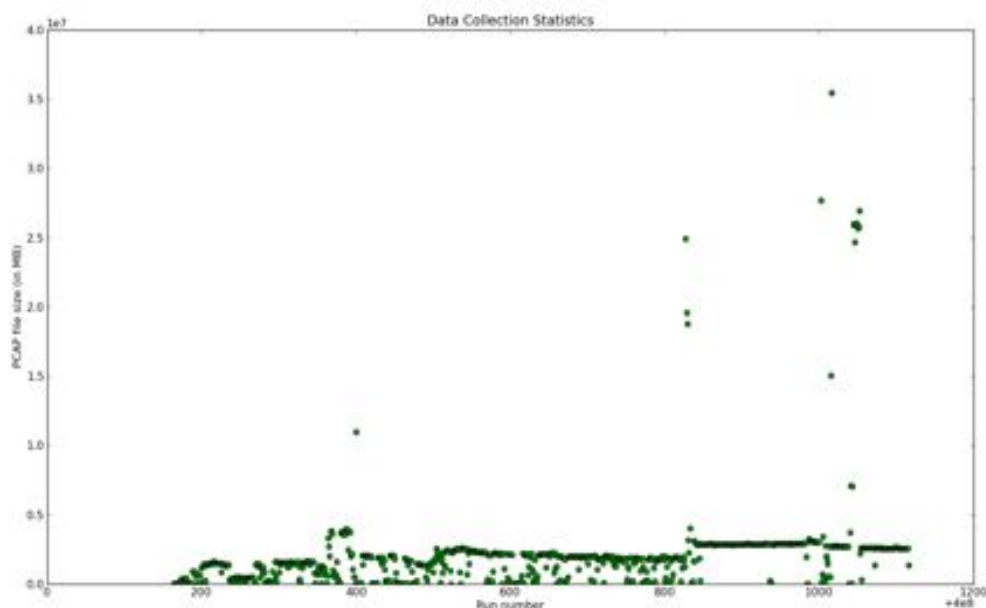


Figure 43: Shown here are the data statistics versus run number.

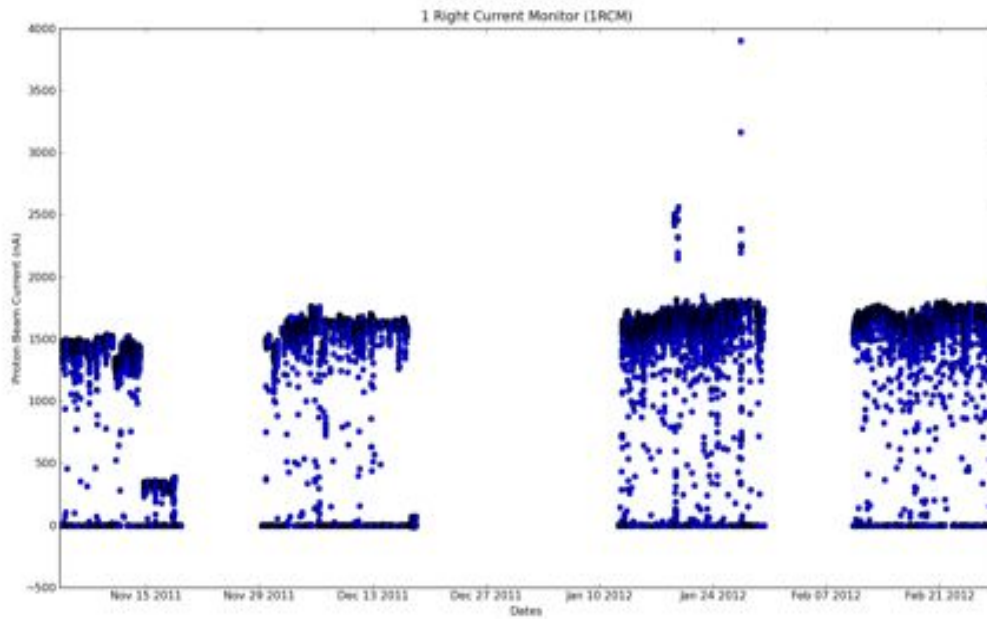


Figure 44: Shown here is the beam current monitoring at the 1 Right path..

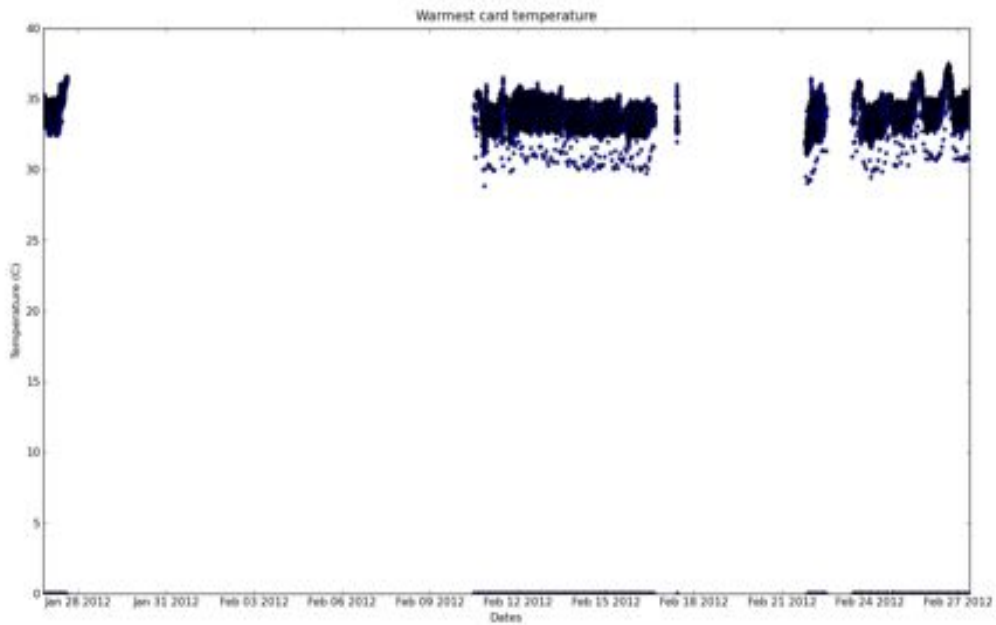


Figure 45: Shown here is the warmest EtherDAQ card temperature variation during data taking.

TPC Data Analysis

The particle ionization characteristic from both Pu and Uranium data has been studied to better understand the detector performance, such as the space charge effect from the track density inside the TPC gas volume. Figure 46 shows the specific ionization of alpha tracks from both data set. The overall shape of the ionization along the track looks similar while difference shows at the beginning part of the track. The dE/dx shape is lower near the start part of the alpha track from Pu data compared to the alpha track from Uranium data. It could due to some kind of attenuation of drift electrons by gas ions created from high density tracks per unit time for the Pu compared to Uranium. The effect seems to be most significant at the beginning of the track where the drift electrons travel the longest distance to pad plane. Similar effects may be present in recoil proton and fission fragment events but is not distinct for the much smaller deposit energy of proton and the more complicated space charge effect of the fission fragment.

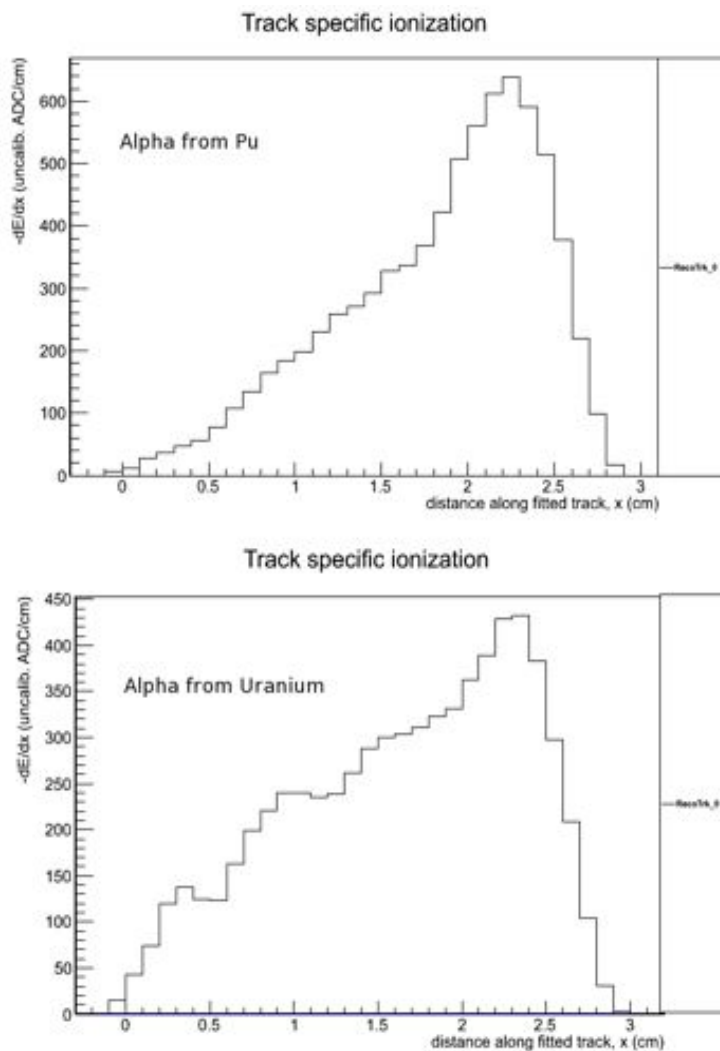


Figure 46: Shown here is the deposited energy per unit length along the reconstructed track of the alpha from the Pu and Uranium data.

Particle identification studies

The Uranium data set has been analyzed to check and compare the track ionization for the different types of produced particles. Before applying any calibration, the relative ADC comparison is used to identify and separate the types of particles. An identified proton track is shown in Figure 47. The dE/dx shows the peak ionization energy is around 100 ADC/cm. The discontinuity of shape of the specific ionization along the track is due to dead channels in the TPC. An alpha track is identified in Figure 48. The track ionization peak is about 500 ADC/cm. In Figure 49, a fission fragment track is identified by the peak ionization energy at the several thousand ADC/cm level. The large charge tail appears at the start position of the real fission track in this image.

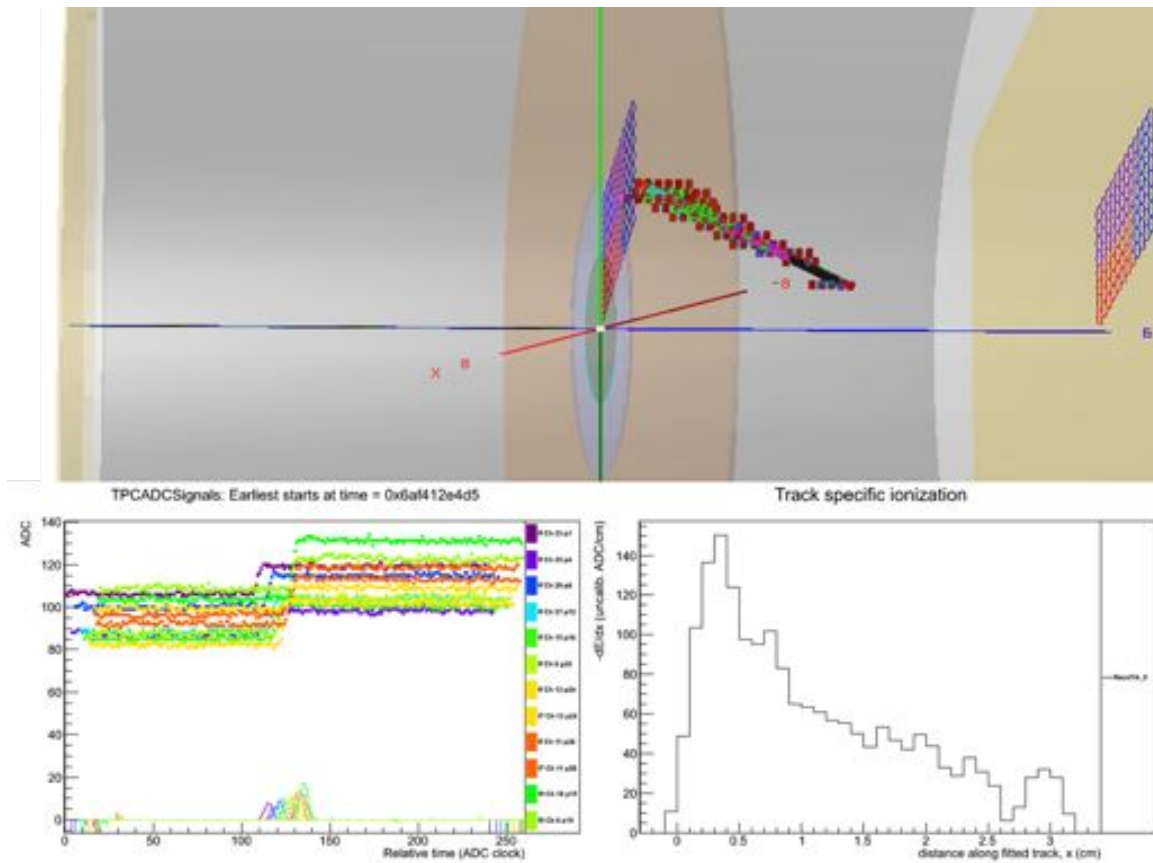


Figure 47: dE/dx of an identified proton track showing peak ionization.

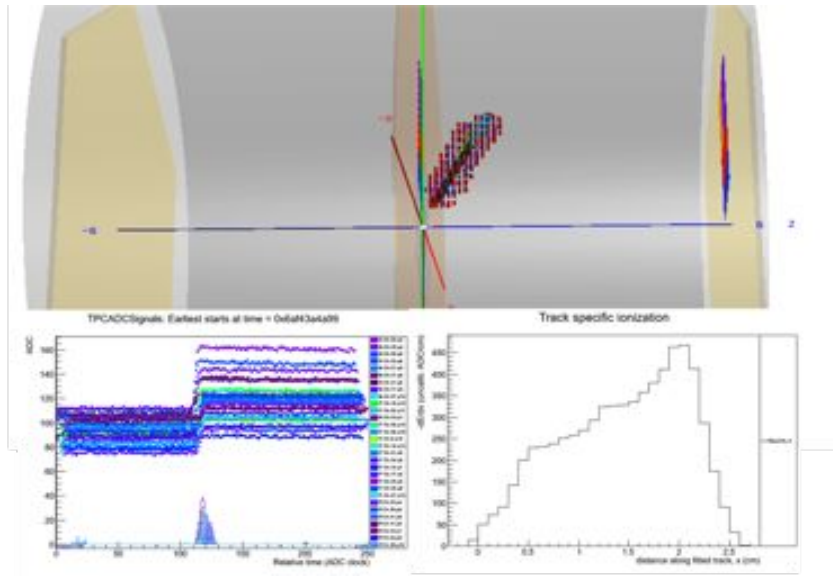


Figure 48: dE/dx of an identified alpha track showing peak ionization.

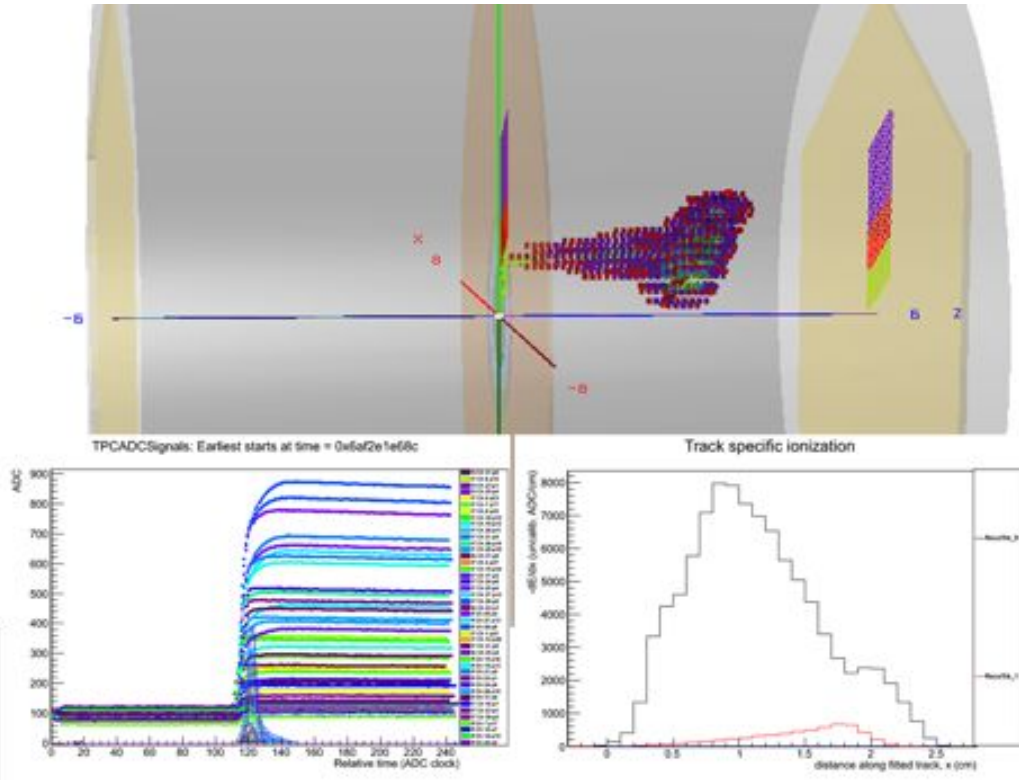


Figure 49: dE/dx of an identified fission fragment showing peak ionization.

The Hydrogen Standard [OU]

Scope

The project to accurately and precisely determine fission cross sections hinges on the H(n,n)H total cross section and angular distributions. The H(n,n)H total cross section is well determined with errors less than 0.5%. In the planned TPC measurements, hydrogen will be used as the working gas for a new standards measurement of U-235. The H(n,n)H angular distribution must be known to connect the total cross section to the measured elastic recoils in the TPC.

Highlights

- High accuracy neutron detector calibrations are underway.

Hydrogen Standard

The TPC offers a major advance in technology for measuring the H(n,n)H angular distribution. The solid angle for this detector is a factor of 100 larger than that used in our current measurements at 14.9 MeV. The target thickness would be comparable. This would result in a counting rate increase by a nearly a factor of 100. This may allow high accuracy measurements of the angular distributions. A further factor is that the beam need not be as strongly collimated which would give as much as another factor of 10 in statistical improvement. This may reduce the experimental running time for a 1% measurement from 3 months to days. The fitted angular distribution can then be compared to calculations based on potential models such as Bonn or on phase shifts such as Arndt. This may eventually provide a test of the QCD-based model of nuclear forces. We are proposing to collaborate on the modeling of hydrogen scattering in the TPC chamber. We will look at the minimum energy detected. We will also investigate the angular resolution for H(n,n)H scattering in the chamber. A pure hydrogen atmosphere will be investigated along with addition of quenching and/or scintillating gases. Further work will also be done on determining the gas composition and density to better than 0.2%. The systematic errors in a standard measurement must be fully explored in order to reach the desired goal. The modeling work will be focused on these problems. Consideration will also be given to possible inter-comparison of the neutron standards such as ${}^6\text{Li}(n,\alpha){}^3\text{H}$, ${}^{10}\text{B}(n,\alpha){}^7\text{Li}$ and ${}^{235}\text{U}(n, f)$.

Neutron Detector Calibration

We are working on calibration of a neutron detector to 1-2% error in the efficiency using a Cf-238 fission chamber. A measurement of a Cf-238 in a fission chamber has been in progress for over 2 months with good stability. We are investigating some changes that occurred when a pulsed deuteron beam was delivered to another beam leg. This detector will be used in the H(n,n)H scattering experiments and in symmetric nuclear reactions to extend the efficiency range from 0.020 MeV to 20 MeV with similar accuracy.

Facilities and Operation [LANL, LLNL, OU]

Scope

Due to the necessity to have a finely tuned neutron beam, with as little contamination as possible, the experimental area needs to be groomed for TPC installation and running. This will mean additional collimation will be needed to adjust the 90L flight path to work with the TPC. MCNPX simulations will be made of the 90L flight path.

The TPC mount will need to be fabricated. The TPC mount will consist of a 3-axis positioner that the TPC will mount to that will allow for precise positioning of the TPC in the neutron beam. The design specifications will come from the TPC design team, as well as 3 axis movement specifications for fine-tuning in the LANSCE beam. The experimental infrastructure will be partially provided by facilities currently at the LANSCE facility. A good working rapport has been established with the facilities personnel at LANSCE through this collaborative effort.

The TPC experiment will be maintained and monitored while located at LANSCE. The Nuclear Science group employs a number of qualified technicians who will perform the required upkeep and maintenance of the TPC and related systems. The facilities will be maintained to that the instrument will function properly and beams can be supplied to the area. The TPC detector and associated electronics will be maintained as necessary. The gas system will be monitored and maintained, including gas bottle replacements and any required periodic testing. The data acquisition system will be maintained by experimenters and a LANSCE supplied computer technician.

In addition to running at LANSCE, the TPC will also run at other facilities to cross check systematic errors. This will be critical to achieve the small systematic errors that are the goal of this experiment. One possibility is the ALEXIS facility under construction at LLNL. This mono energetic neutron source is notable for the low cost (\$150/hr to have the whole facility) and high luminosity (10^8 n/s at 10 cm) neutron beam that will complement the LANSCE facility.

Another notable resource is the accelerator at Ohio University, which will be used to study the hydrogen standard for this project and develop the data required to extend the small uncertainties in the H(n,n)H total cross section to the actinide measurements.

Highlights

- The WNR construction work is complete and the 90L flight path has been reconfigured for the upcoming run cycle.

Livermore [LLNL]

There are numerous facilities at LLNL that are of interest to this project. The construction of ALEXIS, Accelerator at Livermore for EXperiments in Isotope Sciences, is still being considered. This facility will generate pseudo-monoenergetic neutrons up to 10^8 n/s/cm² at energies from 100keV up to 14MeV at low operating cost. The LC computing system has large CPU clusters and storage systems that have been successfully utilized by similar computing projects such as Phenix at RHIC, MIPP at FNAL, and is currently working on setting up ALICE at CERN.

TPC Laboratory Improvements

Expanded the TPC lab space at LLNL by 50%. Work on the lab infrastructure includes new A/C units, which slowed lab work on the TPC this quarter.

Los Alamos [LANL]

The Nuclear Science group at Los Alamos Neutron Science Center operates and maintains the Weapons Neutron Research facility that provides spallation neutrons to five flight paths. The group also maintains and operates two moderated neutron flight paths in the Lujan Center. The group operates and maintains the Blue Room facility, with access to an 800 MeV proton beam and a Lead Slowing Down Spectrometer. The Nuclear Science team will provide the floor space and neutron beam access to the TPC project primarily on the 90Left flight path at the WNR and flight path 5 of the Lujan Center. The 90L flight path experimental area is inside a new construction that contains an overhead crane, light lab space, a vented hood, source safes, computers and easy access to the neutron beam line. Flight path 5 experimental area includes an overhead crane, light lab space, source safes, computers and easy access to the neutron beam line. Recently refurbished light lab space will also be available for TPC work. Monitored stacks are in the vicinity of the two flight paths for TPC gas system and hood exhausts. Radiological shipments and handling facilities are also available. The LANSCE facility provides outside users with all necessary training, a cafeteria and meeting rooms.

WNR Construction and 90L Flight Path Reconfiguration

The construction of a new building that will cover a large part of the WNR south yard is nearly complete (Figure 50, Figure 51). The area is no longer considered a construction site, and only minor tasks (additional emergency lighting, signage, etc.) remain. WNR scientists are expected to obtain full occupancy of the building in mid-June.



Figure 50: View of new building from WNR south yard.



Figure 51: Interior view of the new WNR building.

The 90L flight path was reconfigured to reduce room return and allow experimenters to more easily access equipment. The new flight path, widened from 6 feet to 9.5 feet, is shown in Figure 52. Since the TPC will now be placed closer to the shutter position, all in-room collimation has been removed. The flight path is completely accessible to experimenters and has been cleaned and organized for the 2012 run cycle.

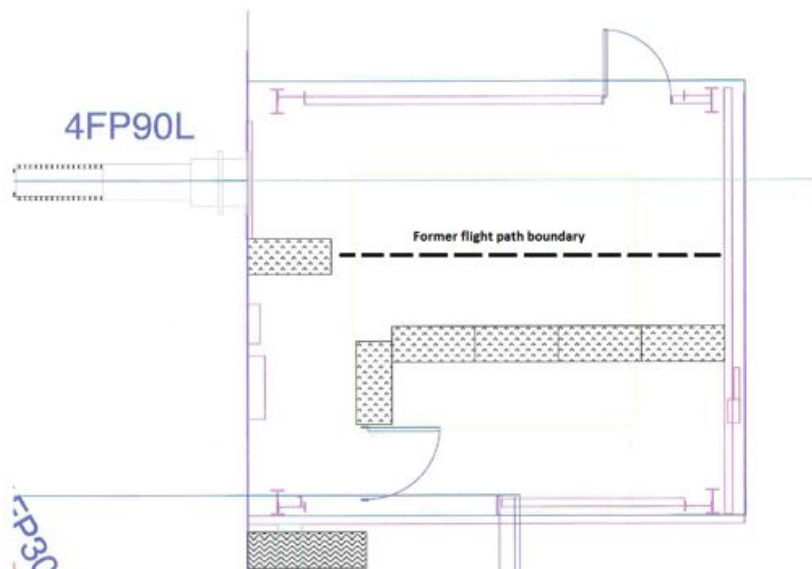


Figure 52: Schematic of reconfigured flight path. Dashed line indicates where shielding blocks were prior to the reconfiguration. Dotted rectangles indicate current location of shielding blocks.

2012 LANSCE Run Cycle

The LANSCE Program Advisory Committee met in April to consider beam time allocation in the 2012 LANSCE run cycle (August – December 2012). The TPC collaboration submitted four proposals. One development proposal, to test the integration of new hardware and software capabilities, and three proposals to investigate the U238/U235, Pu239/U235, and Pu239/H(n,n) cross-section ratios. All proposals were approved and the 90L flight path at WNR has been dedicated to TPC operations over the full 2012 run cycle.

Several purchases were made to facilitate the 2012 run cycle operations, including a complete set of cooling fans, 100 new fiber-optic cables, and an Uninterruptable Power Source (UPS) system which will reduce electronic noise by isolating the TPC system from the LANSCE power grid. The UPS was funded by the LANL Laboratory Directed Research and Development (LDRD) Office.

LANL Summer Student Contributions

Four summer students have been stationed at LANL to help with the TPC project. Lucas Montoya (NMSU) and Paul Greife (CSU), both undergraduate engineering students, have been assisting with infrastructure developments including: upgrades to the TPC positioning table, cable relief systems to manage fiber optic cables, storage containers for field cages that have been loaded with Pu samples, and installing cooling fans onto TPC shielding. William (Spenser) Lynn (ACU, undergraduate), is testing and developing a plan to turn the glove box purchased in 2010 into a Class-1 clean room environment, to facilitate loading of high-activity samples into the TPC. Dana Duke (CSM, graduate) is returning to LANL for the third summer to upgrade the TPC gas handling system from Windows to Linux operating systems and from Labview to C++ programming.



Figure 53: (From left) LANL summer students Spenser Lynn, Dana Duke, (postdoc) Rhiannon Meharchand, and Paul Greife.

Ohio University [OU]

The work proposed will be undertaken in the Edwards Accelerator Laboratory of the Department of Physics and Astronomy at Ohio University. The laboratory includes a vault for the accelerator, two target rooms, a control room, a thin film preparation and chemistry room with a fume hood, an electronics shop, a teaching laboratory for small non-accelerator based nuclear experiments, and offices for students, staff, and faculty. The Laboratory building supplies approximately 10,000 square feet of lab space and 5,000 square feet of office space. In the Clippinger Research Laboratories, the Department of Physics and Astronomy has a 3000 square foot mechanical shop, staffed by two machinists, that supports all the experimental work of the department. The machinists have numerically controlled machines that they use in the fabrication of apparatus used in experiments, they are accomplished at making parts from exotic materials such as refractory metals, and can perform heli-arc welding and other sophisticated joining techniques.

The heart of the Edwards Accelerator Laboratory is the 4.5-MV tandem Van de Graaff accelerator and six beam lines. This machine is equipped with a sputter ion source and a duoplasmatron charge-exchange ion source for the production of proton, deuteron, ^3He , and heavy ion beams. DC beams of up to 30 μA are routinely available for protons, deuterons and many other species from the sputter ion source. Pulsing and bunching equipment are capable of achieving 1 ns bursts for proton and deuteron beams, 2.5 ns bursts for ^3He beams, and 3 ns bursts for ^7Li . The accelerator belt was replaced most recently in March 2004; the accelerator has performed very well since that time with good stability for terminal voltages up to 4.0 MV. The SF₆ compressor and gas-handling system were refurbished in April 2005. The Laboratory is very well equipped for neutron time-of-flight experiments. The building is very well shielded thus allowing the production of neutrons from reactions such as $d(d,n)$. A beam swinger magnet and time-of-flight tunnel allow flight paths ranging from 4 to 30 m. The tunnel is well shielded, and the swinger-magnet assembly allows angular distributions to be measured with a single flight path.

Tandem Operations

We have completed the conversion of our tandem into a pelletron. We anticipate on months testing before experiments resume. We have reached a terminal voltage of 4.0 MV with 75 PSI SF₆ in the tandem. We will increase the SF₆ pressure to 95 PSI to allow stable operation to higher voltages. We have 15 operators taking refresher training to comply with the new Ohio Department of Health rules for industrial accelerators. We have recently lost the facility chiller due to freezing the heat exchanger, repairs are expected to take at least 3 weeks.

H(n,n)H Scattering Experiment

We produced a $^6\text{LiCl}$ target on a platinum backing and a covering of gold. This will be used for efficiency determination using the symmetric reaction $^6\text{Li} + ^6\text{Li}$. We have begun the setup of the Hydrogen scattering experiment. The ^{252}Cf calibration work to achieve ~2% errors in the efficiency between 1 and 8 MeV is currently underway. We are continuing the preparation work to perform the measurement of $H(n,n)H$ scattering at small neutron scattering angles by measurement of the scattered neutron.

Management

The NIFFTE university collaborators are funded directly by the Advanced Fuel Campaign of the FCT Program. The PI of this contract has reporting responsibilities directly to the Technical Point of Contact at INL. The laboratories are being funded directly by the FCT and ARC programs to not only participate but to provide guidance and project oversight, including reporting requirements within the DOE/NE management system.